

University of Windsor

Scholarship at UWindor

Electronic Theses and Dissertations

Theses, Dissertations, and Major Papers

2019

Simulation of Pipe Hydroforming

Yang Jin

University of Windsor

Follow this and additional works at: <https://scholar.uwindsor.ca/etd>

Recommended Citation

Jin, Yang, "Simulation of Pipe Hydroforming" (2019). *Electronic Theses and Dissertations*. 7710.
<https://scholar.uwindsor.ca/etd/7710>

This online database contains the full-text of PhD dissertations and Masters' theses of University of Windsor students from 1954 forward. These documents are made available for personal study and research purposes only, in accordance with the Canadian Copyright Act and the Creative Commons license—CC BY-NC-ND (Attribution, Non-Commercial, No Derivative Works). Under this license, works must always be attributed to the copyright holder (original author), cannot be used for any commercial purposes, and may not be altered. Any other use would require the permission of the copyright holder. Students may inquire about withdrawing their dissertation and/or thesis from this database. For additional inquiries, please contact the repository administrator via email (scholarship@uwindsor.ca) or by telephone at 519-253-3000ext. 3208.

Simulation of Pipe Hydroforming

By

Yang Jin

A Thesis

Submitted to the **Faculty of Graduate Studies**
through the Department of
Mechanical, Automotive and Materials Engineering
in Partial Fulfillment of the Requirements for
the Degree of **Master of Applied Science**
at the **University of Windsor**

Windsor, Ontario, Canada

2019

© 2019 Yang Jin

Simulation of Pipe Hydroforming

by

Yang Jin

Approved by

X. Xu

Department of Civil & Environmental Engineering

E. Lang

Department of Mechanical, Automotive & Materials Engineering

L. Oriet, Advisor

Department of Mechanical, Automotive & Materials Engineering

April 26, 2019

DECLARATION OF ORIGINALITY

I hereby certify that I am the sole author of this thesis and that no part of this thesis has been published or submitted for publication.

I certify that, to the best of my knowledge, my thesis does not infringe upon anyone's copyright nor violate any proprietary rights and that any ideas, techniques, quotations, or any other material from the work of other people included in my thesis, published or otherwise, are fully acknowledged in accordance with the standard referencing practices. Furthermore, to the extent that I have included copyrighted material that surpasses the bounds of fair dealing within the meaning of the Canada Copyright Act, I certify that I have obtained a written permission from the copyright owner(s) to include such material(s) in my thesis and have included copies of such copyright clearances to my appendix.

I declare that this is a true copy of my thesis, including any final revisions, as approved by my thesis committee and the Graduate Studies office, and that this thesis has not been submitted for a higher degree to any other University or Institution.

ABSTRACT

The importance of investigating the formation of a torsion beam and understanding how it can be manipulated to perform at an optimum condition is crucial to car manufacturers. Developing and remodelling the torsion beam can allow both a simpler structure and quicker assembly while reducing the space required for a car suspension's system, thus saving time and costs for manufacturers.

Nowadays, the use of hydroforming technology has become widespread because it is able to obtain complex hollow parts more easily and has been continually developed to become a globally applied technology in the formation of a torsion beam of a vehicle.

With regards to the current issues in academic research and real-world production, this research uses a finite element analysis (FEA) method-based software tool DYNAFORM, to simulate the pipe hydroforming process in order to show the overall manufacturing process, thus providing a precise FEA simulation model of a torsion beam suspension for the automotive manufacturing. This will also provide a math model (a regression equation) for further research and the further application of this technology in the future.

DEDICATION

To my family,

Thank you for the support, understanding and your selfless love.

ACKNOWLEDGEMENTS

I would like to thank those who helped me whilst I was studying the MASc program at the University of Windsor.

My committee members, thank you all for your kind help and professional advice during my study. Dr. L. Oriet, as my advisor, you supervised, helped and advised me throughout the time during this program. Dr. E. Lang, as my program reader, thank you for your valuable and professional advice every time when I asked for your assistance. Dr. X. Xu, as my outside reader, thank you for your patience and support throughout.

I appreciate Longchang Shanchuan Precision Welded Pipe Co. Ltd. for giving me this amazing opportunity to work and finish my master's research at his manufacturing, research and development facility. Mr. Lv, a special thanks to you, thank you for your trust and your supervision at the company, and also your diligent guidance which helped me to finish the project smoothly.

Finally, I thank my family for their unconditional and selfless love. I love you all very much, and I know I could not make it this far without you all.

TABLE OF CONTENTS

DECLARATION OF ORIGINALITY	iii
ABSTRACT	iv
DEDICATION	v
ACKNOWLEDGEMENTS.....	vi
LIST OF TABLES.....	ix
LIST OF FIGURES	x
Chapter 1 Introduction.....	1
1.1 Backgrounds and Research Outline	1
1.2 The Torsion Beam Suspension	3
1.3 Project Overview	6
Chapter 2 Theory and Literature Review.....	9
2.1 Basic Theory and Practical Characteristics.....	9
2.2 Research Status and Development Trends.....	11
2.2.1 Backgrounds of Research.....	11
2.2.2 Development Trends	14
2.3 Overview of Torsion Beam Tube Hydroforming Process	15
2.3.1 The Squeezing Composite Forming Method	15
2.3.2 The Squeezing Separation Forming Method.....	17
2.3.3 Hydroforming Method	18
2.4 Automotive Tubular Torsion Beam Forming.....	18
2.5 Torsion Beam Tube Hydroforming Analysis Method	20
2.6 Main Factors Affecting the Formation of Automotive Tubular Torsion Beam	22
Chapter 3 FEA Simulation Software Tools.....	25
3.1 Finite Element Analysis	25
3.2 DYNAFORM for Metal Forming	27
3.3 Main Features of DYNAFORM.....	29
Chapter 4 Methodology	30
4.1 Torsion Beam Finite Element Model.....	30
4.2 Torsion Beam Material	30
4.3 Simulation Factors	32

Chapter 5 Results	37
5.1 Simulation Results.....	37
5.2 Mathematical Model	40
5.3 Significant Factors	42
5.4 Model Summary	44
5.5 Scatterplots	46
Chapter 6 Conclusions and Future Research.....	50
6.1 Conclusions	50
6.2 Future Research	51
Reference.....	53
Appendices.....	57
Appendix A Technical requirements of the torsion beam.....	57
Appendix B Regression Analysis.....	58
Appendix C Regression Analysis – Regression Plots 2D.....	59
Appendix D Regression Analysis – Regression Plots 3D.....	60
Appendix E Regression Analysis – Residual Plots	61
Appendix F General Factorial Regression with 54 Runs	62
Appendix G General Factorial Regression – Plots.....	65
Vita Auctoris	69

LIST OF TABLES

Table 1. Equation variables.	31
Table 2. Three factors with different levels.....	34
Table 3. DYNAFORM simulation results.....	39
Table 4. MINITAB worksheet.....	41
Table 5. ANOVA (analysis of variance).....	43
Table 6. Percentage contribution of sum of square.	44
Table 7. Model Summary.	45

LIST OF FIGURES

Figure 1. Non-independent suspension.	3
Figure 2. Independent suspension.	3
Figure 3. U shape and V shape of torsion beam cross-sectional area.	4
Figure 4. Photoshoot of Longchang Shanchuan Precision Welded Pipe Co. Ltd.	6
Figure 5. 2D drawing of the front view of the torsion beam.	8
Figure 6. Technical requirements of the torsion beam.	8
Figure 7. Punches - squeezing separation forming method.	17
Figure 8. FEA model in DYNAFORM.	30
Figure 9. CP800 stress-strain curve.	31
Figure 10. Tube sealing prior to stamp cycle.	35
Figure 11. Scatterplot of thinning rate vs P.	46
Figure 12. Surface plot of thinning rate vs T.	47
Figure 13. Surface plot of thinning rate vs P, T.	48
Figure 14. 3D scatterplot of thinning rate vs P vs T.	49

Chapter 1 Introduction

1.1 Backgrounds and Research Outline

In the 21st century, with the continuous innovation and research and application of industrial manufacturing technology, the forming technology has developed rapidly [1].

The hydroforming technology of pipe fittings has become very popular in advanced forming technology. Especially in the automotive industry, many assemblies, pressure weldments and body frames can be replaced by lighter, stronger, more precise and less expensive hydroformed parts [2].

Compared with traditional casting (solidifies the liquid metal from a mold), welding (joins metals by applying high heat), stamping (forms a sheet metal into a required shape by stamping press), forging (shapes metal by applying compressive forces) and machining (cuts raw materials into desired shapes) processes, the hydroforming technology of pipe fittings uses bending, partial forming, bulging or extrusion and bulging composite forming processes to form the pipe, which is able to obtain complex hollow parts easier. Parts produced by this method are preferred over conventional processes due to many advantages, such as more accuracy and less springback [3], so the tubular hydroformed parts have been used more and more widely. They can replace some forgings, castings and welded parts, and are widely used in aerospace [4], automobiles, office equipment, household appliances, etc., which also have brought significant

economic benefits, because they can reduce the usages of materials. Therefore, the research of this technology has become a key focus area.

The outline of this research is as follows:

- (1) Numerically simulate the tubular hydroforming process of a torsion beam by using the finite element software tool, DYNAFORM. DYNAFORM will be applied to simulate the forming process of turning a tube into a torsion beam, thus the numerical data obtained will serve to formulate the final results.
- (2) Collect the individual results of the data (thinning rate) for each simulation in order to determine which simulations can be considered successful.
- (3) Generate a math model and a regression equation in MINITAB. This model and equation will function as a guide in predicting and also verifying the accuracy of the thinning rates in the actual manufacturing processes.
- (4) Analyze the collecting data (thinning rate) and determine the most significant factor in the experiment based on the collected data.
- (5) Determine the optimal setting (a combination of the pressure, the mesh and the loading time) for the manufacturing process.

The purposes of the research on this subject are to find out the significant factors affecting the forming results, and to obtain the relationship between these factors and the forming results through numerically simulating the torsion beam. Then by applying the

tube hydroforming process and getting the best settings for the parameters, which improve the process technology of the system, this automated method will be promoted and applied in the actual manufacturing processes.

1.2 The Torsion Beam Suspension

The suspension of an automobile is a crucial part of the vehicle. The suspension is the general term for all power transmission connections between the axle (or wheels) and the frame (or load-bearing body). The torsion beam is a semi-independent suspension. Strictly speaking, the suspension has only two types, which are non-independent (Figure 1) and independent (Figure 2).

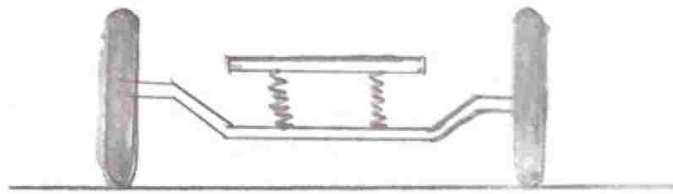


Figure 1. Non-independent suspension.

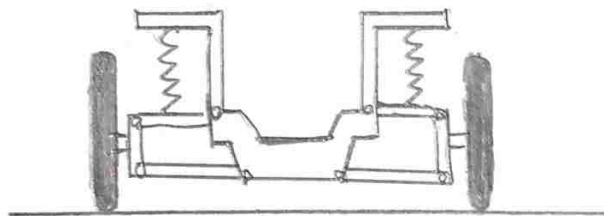


Figure 2. Independent suspension.

However, the torsion beam suspension is different from the non-independent suspension on passenger cars, vans, minivans, so it is usually also called by another title, semi-detached suspension [5]. The trailing arm torsion beam suspension consists of two longitudinal swing arms and a torsion beam that can be twisted, and the springs and shock absorbers are generally placed at the rear end of the trailing arm near the wheel bearing housing. The cross-sectional area (by cutting from the middle) of the beam can be basically divided into two categories: open and closed. The open can be V-shaped or U-shaped (Figure 3). The beam is formed by stamping to form a torsion beam with variable cross-section, since there is not stamped at all at the original cross-sections, so as to improve the rigidity of both ends to maintain the stability [4].



Figure 3. U shape and V shape of torsion beam cross-sectional area.

The main functions of the suspension system are: [6]

1. Mitigating the impact of the road on the vehicle
2. Attenuating the vibration between the vehicle body and the wheels
3. Transmitting the force between the wheels and the road
4. Controlling the movement posture of the wheels and the body

5. Ensuring the normal running of the vehicle maintain adequate tire contact with the road surface under all driving conditions.

The advantages of a trailing arm suspension system are that, since the entire system consists of only one large component, the structure is simpler than the complicated double wishbones, multiple links, and so on. The trailing arm suspension is mounted on the body as a whole [8], and the rocker arm has only two connection points to the body, so the assembly is also simple, and the cost is low, which is what this level of vehicle needs. In addition, the space occupied by the trailing arm suspension as a whole is relatively small. The disadvantages of the suspension system include poor bearing performance, weak anti-rolling ability, poor performance of good shock absorption, and limited comfort level. Because the trailing arm suspension operates in a manner that is close to a non-independent suspension [9], its shock filtering resistance or controllability is far less than a traditional independent suspension.

Therefore, it is very important and useful to analyze the formation of a torsion beam suspension. This thesis will provide a precise reference model for a torsion beam suspension simulation in the future automotive manufacturing. This model can precisely predict the desired results (thinning rates and the final form of the torsion beam) through the use of FEA simulation. As a result, the reference model also saves time and cost in the actual mass production process.

1.3 Project Overview

The project is offered by a company called **Longchang Shanchuan Precision Welded Pipe Co. Ltd.**, and the author was working there as a Co-Op student.



Figure 4. Photoshoot of Longchang Shanchuan Precision Welded Pipe Co. Ltd.

The company is an auto parts enterprise integrating scientific research, design, production and sales. The company is located in the “Sichuan and Chongqing Economic Cooperation Experimental Demonstration Zone” in Longchang City, Sichuan Province, China. The area has both a convenient transportation infrastructure and skilled workers. The company covers an area of 63,0000 m² and has more than 900 employees and was founded in 1965. In recent years, professional level and mature technology in the field of precision welded pipe and vehicle damper, the company has rapidly emerged in the specialty field of auto parts.

The author was given total responsibility for the research project work, and the work will be used for the real-world manufacturing process by the company and also his own master thesis writing.

This model was built by the software tool, DYNAFORM, which is a finite-element based software tool. The model is simulating a torsion beam which nowadays is widely used in the semi-independent suspension systems [10]. Since the structure of a torsion beam is simple and does not require too much space, it is often used in the rear suspension system of a front-wheel drive vehicle because its low cost.

Before the simulation gets started, the company would receive a basic CAD model and a 2D sketch file of the designated product from the customer. These files would then be used as a reference to define the project in the end. For example, the CAD files included the geometries of the torsion beam (final shape) and the dies. The shapes of dies would not change, and they would be considered as rigid parts during the simulation. The 2D drawings of the multiple views of the torsion beam, and also the cross-section views of the torsion beam are shown below. By observing the 2D drawings (Figure 5), we can find that the required length of the torsion beam, as well as the tube blank at the beginning is 1177.6 mm, the required diameter is 101 mm, the required thickness is 3.5 mm, and required material is CP800, which is a complex phased steel.

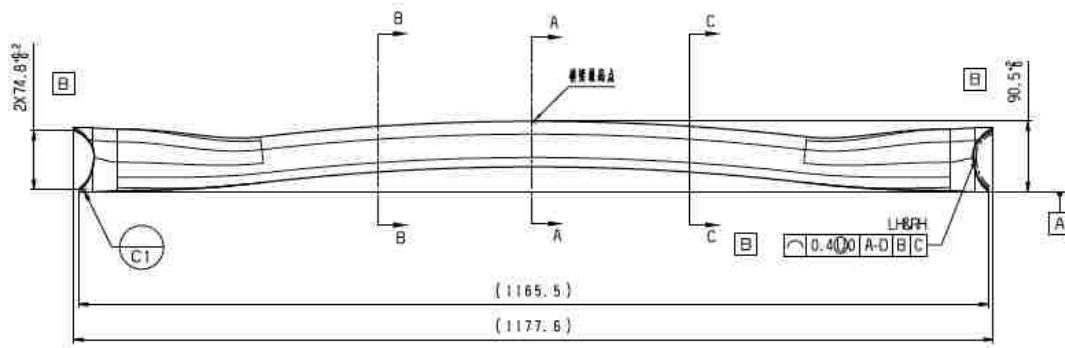


Figure 5. 2D drawing of the front view of the torsion beam.

Meanwhile, the CAD model files can be opened in CATIA (a multi-platform software tool for computer-aided design), and also will be used in DYNAFORM (introduced in Chapter 3) later on. However, the original shape of the torsion beam, a regular tube, will be created in CATIA. As for the 2D files, they will provide all the details, such as the multi-side views, the boundary conditions, technical requirements (Figure 6), etc.

技术要求	Technical Requirements
1 未注尺寸见数模	1. See the digital model for unmarked dimensions
2 未注线性尺寸公差为 ± 0.5	2. Unmarked linear tolerance is ± 0.5
3 未注角度公差为 $\pm 1^\circ$	3. Unmarked angle tolerance is $\pm 1^\circ$
4 所有线轮廓度为 $\sqrt{0.4(0) A-D B C}$	4. All line profiles are $\sqrt{0.4(0) A-D B C}$
5 未注面轮廓度为 $\sqrt{0.4(0) A-D B C}$	5. The contour of the surface is $\sqrt{0.4(0) A-D B C}$
6 成形后材料减薄率不得大于10%	6. The material thinning rate after molding should not exceed 10%

Figure 6. Technical requirements of the torsion beam.

Please note that design requirement #6 is a critical dimension, this because it is the determining factor of whether the results can be considered acceptable.

Chapter 2 Theory and Literature Review

2.1 Basic Theory and Practical Characteristics

Tube Hydro-forming (THF) is a unique forming process. Firstly, the tube blank is placed into the die, then the tube is filled with high-pressure liquid, which supplements the tube with axial pressure to make the diameter expand, and finally the dies are closed. Pipe hydroforming technology (also known as net forming technology, internal high-pressure forming technology or hydraulic bulging technology) uses a combination of bending, partial forming, bulging or extrusion composite forming process to plastically form the pipe to obtain various complex hollow members. Compared with the traditional machining, stamping, casting, forging, welding and other processes, THF technology has the following advantages [12]:

1) Reducing weight

Since the complex-shaped parts can be formed at one time, the number of structural parts and the welding weight are reduced, and less raw materials can be used, so the hydroforming technology has a significant weight reduction effect. Compared with stamped and welded parts, the hollow structural parts produced by hydraulic forming technology can reduce the weight. Also, there are no weld flanges since the entire hydroformed part is made of structural tube. This eliminates the double metal thickness needed for welding, the weight resulting from the double metal thickness and all the

labour that goes into fixturing and welding separate C channels to form an equivalent hollow member.

2) Reducing the number of semi-finished parts

According to statistics, compared with stamped and welded parts, the hydroforming technology can reduce the number of parts of the sub-frame of the car, as well as all the cumulative costs of manual labour, material handling and the assembly process. Thus, there are a lot of savings when hydroforming tubular parts.

3) Reducing the cost of the dies

Reducing the number of parts can reduce the number of dies, which can save the cost of designing and manufacturing dies themselves.

4) Flexibility and innovation

It can overcome the limitations of traditional manufacturing processes and be applied to the design and development of new products. It is precisely because of the above advantages that hydroforming technology has been increasingly used in the automotive, aerospace, marine, home appliances and other industrial fields. At present, the developed countries of the automobile industry such as United States, Germany, Japan, South Korea, etc [13].

2.2 Research Status and Development Trends

THF technology began in the 1940s when it was mainly used to form T-tube joints [11]. By the end of the 1970s, Germany began basic research on THF technology, and in the early 1990s, the technology was first applied to produce automotive structural parts [14]. THF technology is a relatively new manufacturing technique compared to conventional stamping processes. Currently, many research institutions have carried out a lot of study on this technology from different aspects, such as forming mechanism, pipe selection, friction characteristics, preform design, forming process, die material and coating treatment.

2.2.1 Backgrounds of Research

1. Theoretical and experimental research

The main forms of failure of pipe hydroforming are wrinkling, buckling and cracking. Muammer Koç used plastic theory and thin film theory to establish an analytical model of three failure modes in hydroforming of pipes [15]. He predicted the forming process parameters such as internal pressure, axial pressure, back pressure and wall thickness reduction, which are fundamentally consistent with the experimental results. Although the analytical model has certain limitations and fails to effectively predict the forming limit of complex parts, it has a certain guiding role in the design of hydraulic forming parts, finite element numerical simulation analysis, and understanding of process

parameters. Imanejad experimented on the bulging of aluminum extruded tubes with axial compression and no axial compression, indicating that the forming limit of the latter is significantly greater than the former [16]. Fuchizawa S. studied the stress-strain relationship of the hydroforming of the pipe based on an experimental device with one end fixed and the other end freely movable [17]. The influence of the strain hardening index n and the anisotropy index γ on the pipe forming was discussed in depth. The results show that the value of n increases, the internal pressure required for the tube to swell to a certain height increases, and the forming limit also increases. The obtained wall thickness is more uniform; the circumferential γ value will affect the ultimate bulging pressure (final pressure), while the axial γ value has a greater influence on the maximum bulging ratio [17]. Atsushi Shirayori studied the deformation law of the free bulging of the pipe with the initial wall thickness deviation in the circumferential direction [18]. It is concluded that the degree of deviation of the pipe wall thickness increases with the increase of the degree of bulging.

2. Finite element numerical simulation

The finite element numerical simulation technology can effectively simulate the flow of metal in the hydroforming process of pipes, reveal the stress and strain distribution, wall thickness and profile changes. These reflect the influence of different process parameters on the forming process and predict and analyze the mechanism defect generation. Also, by adjusting the parameters to control the defects, providing scientific basis for the

optimization design of the process and the dies thus saving time and reducing the cost of the trials and error methods, it has been highly valued by researchers and industry. With the development of finite element theory and computer technology, many excellent finite element analysis software tools, such as DYNAFORM, ABAQUS, and CATIA have been created.

3. Hydroforming equipment

The hydroforming equipment consists of a clamping hydraulic press, a horizontal push cylinder, a high-pressure source, a hydraulic system, a hydraulic system and a computer control system. The main functions of each system are: 1. the clamping hydraulic press provides the clamping force, during the pressure forming (creating from the stamping die), the upper and lower dies are closed and locked. 2. the horizontal cylinder is used for axial feeding and tube end sealing. 3. the high-pressure source is used for generating and controlling high-pressure liquid, and the core component is supercharger, specifications are 200MPa, 400MPa and 600MPa [3]. 4. hydraulic power system provides horizontal cylinder, supercharger and clamping hydraulic drive power. 5. hydraulic system provides workpiece forming emulsion fast filling, supercharger high pressure chamber rehydration, and emulsion circulation filtration. 6. computer control system controls horizontal cylinder feed and supercharger internal pressure to form the required internal pressure and displacement loading curve [19]. Presently, many companies and research institutes have developed hydraulic forming equipment. Two important factors to consider when

using hydroformed equipment to produce hydroformed parts are forming cycles and precise control mechanisms [20].

2.2.2 Development Trends

Pipe fitting hydroforming methods have different names in different time periods and countries. Depending on different time and country, it could be known as Bulge Forming of Tube (BFT) and Liquid Bulge Forming (LBF) [21]. For a while, Hydraulic Pressure forming (HPF) was also studied and used by some researchers. In Germany, the manufacturer refers to this process as Internal High Pressure Forming (IHPF) [22].

Although the pipe forming process was used in actual industrial production for only a few decades, the development of this technology and the establishment of its theoretical system can be traced back to the 1940s [23]. Nowadays, the simulation of hydroforming process by finite element method has become an important means for many scholars to study and verify theoretical analysis [24]. Using large finite element software tools, such as DYNIFORM, ABAQUS, CATIA, etc. to simulate the forming process [25]. The deformation of the pipe during the bulging process, such as the excessive thickness of the pipe wall thickness; whether there are instability phenomena, such as buckling and wrinkling; and the forming limit of the pipe under a specific loading path are predicted to formulate a reasonable loading path and design a reasonable die shape. In order to shorten

the development time of the forming process and reduce the development cost, the finite element simulation itself is constantly developing.

2.3 Overview of Torsion Beam Tube Hydroforming Process

The torsion beam tube hydroforming process is an asymmetrical spatial three-dimensional deformation process [26], but the forming process is more complex. In the forming process, the most important forming force is the internal pressure acting on the inside of the tube blank. The forming method of the torsion beam member can be mainly divided into the following three types [26]: the squeezing composite forming method, the squeezing separation forming method and the hydroforming method.

2.3.1 The Squeezing Composite Forming Method

The squeezing composite forming process fills the interior of the tube blank with the hydraulic fluids, and the extrusion punch acting on both ends of the tube blank seals the medium in the inner cavity of the tube blank [27]. During forming, the extrusion punch extrudes the hydraulic fluid to change its volume to produce internal pressure. Therefore, the magnitude of the internal pressure is completely dependent on the movement of the extrusion punch. In this method, the cavity cannot be refilled, or the extra liquid is removed during the forming process, so it is only suitable for torsion beam members with certain geometric features. However, this forming method has advantages, such as a

simple punch structure, less equipment and devices, convenient operation [28], and also, the advantages that the wall thickness of the workpiece is relatively uniform and stable, and the variation range is small. Thus, when the cavity is sealed, there is a negative feedback effect between pressure and volume. This occurs if the volumetric compression of the hydraulic liquid is increased, the internal pressure is increased, the wall of the tube is thinned, the outer diameter of the medium is increased, the volumetric compression is reduced, and the internal pressure is decreased. Conversely, if the volume compression is reduced, the internal pressure is reduced; the pipe wall is thickened, and the outer diameter of the shield is reduced; the volume is reduced, and the internal pressure is increased. This feedback effect is strong and depends directly on the volumetric compression characteristics of the hydraulic liquid.

For the extrusion composite forming, the dimensional relationship of the extrusion punch, the die, the tube blank and the bulging medium determines the initial pressure of the forming. In the forming process, the adjustment of the forming pressure is difficult and can only be carried out within a certain range, primarily by changing the structure of the extrusion punch.

2.3.2 The Squeezing Separation Forming Method

Compared with the squeezing composite forming process, the squeezing and separating forming process has a pair of forming punches in this process, and the internal pressure is generated by a special bulging punch (Figure 7) extrusion forming medium, and the numerical value thereof is the extrusion punch which is independent of the motion of the forming punch [29].

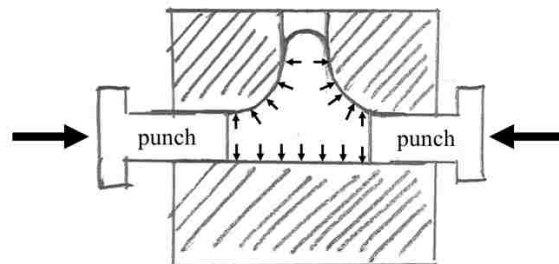


Figure 7. Punches - squeezing separation forming method.

The pressure generation mechanism in this forming process is similar to the squeezing composite forming, but the difference between the two is whether the extrusion punch and the forming punch are integrated. In this forming method, the extrusion punch and the forming punch are driven by a composite cylinder. Compared with the squeezing composite forming, the structure and movement of the punch are more complicated, and the life of the die is low, but the generation and adjustment of the internal pressure during forming is relatively easy, and the sealing requirement of the forming medium is also low.

2.3.3 Hydroforming Method

The principle of the hydroforming method is quite different from the above two forming methods. The main difference is that the internal pressure required for forming is independent of the movement of the punch and is provided by a special hydraulic system, such as a three-stage supercharging system [30].

2.4 Automotive Tubular Torsion Beam Forming

Passenger vehicle weight reduction is a major priority for the automotive industry. The lightweight of the chassis not only helps to reduce fuel consumption, but also greatly improves the comfort of the vehicle. The torsion beam is one of the main components of the chassis. The traditional torsion beam structure is stamped and formed by steel plates [31]. In order to improve the rigidity requirements of the vehicle, it is generally necessary to add a stabilizer bar inside the torsion beam, resulting in an increased weight of the torsion beam assembly. The current method for reducing the weight of the torsion beam is mainly to use a closed variable section tubular torsion beam. The variable-section tubular torsion beam has three forming processes of hydroforming, steel pipe stamping and thermoforming torsion beam, but the forming process cannot be distinguished from the appearance, and the thickness of the steel pipe.

The three forming processes are described as follows:

1. Hydroforming

The liquid medium is injected into the sealed tube blank to generate a high pressure inside, and an axial force is applied to both ends of the tube blank for feeding [32], thus the tube blank material is plastically deformed by an external force [33].

2. Stamp Forming

The pipe is pre-formed, then it will be placed in the die, and the precision control of the die is used to obtain the high-precision pipe parts [34].

3. Hot Forming

The heating pipe is sent to the die, and the parts are cooled by the die water channel while being formed [35].

Compared with the steel plate forming torsion beam, the lightweight effect of the tubular torsion beam is about 15% lighter [36]. The closed tubular structure greatly improves the strength and rigidity of the part, and eliminates the need to install the stabilizer bar, reduce the number of parts, and reduces the comprehensive production of parts cost. Steel pipe stamping and hydroforming are made by welding high temperature and electrical resistant high strength steel materials. The commonly used materials are DP600, FB590, S460MC and so on [37]. In order to improve the strength of the parts, some models use advanced high-strength steel materials such as CP800 and DP800. However, in order to

ensure the quality of the weld, the welded pipe process needs to use the laser welding process. As is used in the welding of hydroformed parts [37].

2.5 Torsion Beam Tube Hydroforming Analysis Method

Torsion beam tube hydroforming is a complex three-dimensional large deformation process [26]. The analysis and research of its hydroforming process are most commonly: firstly, the control of the forming force and the matching relationship during the forming of the tube blank; second, the influence of important process parameters on the forming of the pipe fittings and optimization, in order to improve the forming quality of the torsion beam pipe fittings.

At present, the commonly used method for the study of torsion beam forming process is theoretical research and mechanical analysis [15]. Since the deformation of the torsion beam is complex, large and three-dimensional, and the mechanical analysis derivation does not completely reflect the deformation of the pipe fitting, so the results obtained from the analysis are quite different from the actual experiment. With the rapid development of computer science and the gradual maturity of finite element simulation technology, CAE technology simulation analysis of metal plastic forming process deformation law is more and more widely used in production practice. The successful application of CAE technology [38] cannot only shorten the development cycle of dies

and new products, reduce costs, improve the market competitiveness of enterprises, but also facilitate the combination of finite element analysis and traditional experimental methods. Thus, it promotes the rapid development of modern manufacturing of dies. Therefore, this is the reason for using the special DYNAFORM software to simulate the hydroforming process of a torsion beam, mainly for the loading relationship between the torsion beam forming force and the important parameters affecting the forming of the torsion beam. Several well-developed FEA software tools exist that can do finite element analysis simulation for hydroforming, such as DYNAFORM and CATIA. This research uses DYNAFORM to maintain the consistency with the technology used by Longchang Shanchuan Precision Welded Pipe Co. Ltd., the sponsor in China. DYNAFORM is preferable because it can detect the thinning rate of projects easily and precisely, and the thinning rate is the only determining condition in this project.

2.6 Main Factors Affecting the Formation of Automotive Tubular Torsion Beam

The forming process of automobile tubular torsion beam is a typical three-dimensional large deformation of space. The forming process is complicated and there are many intricacies. The main aspects are as follows:

1. Process Power

In the automotive tubular torsion beam forming process, there are four forces acting; internal pressure, pressing force, balance force and clamping force [39]. The first three are forming forces, and their size and proportional relationship are very important, which directly determines the stress-strain state during the deformation of the pipe. During the forming process, the internal pressure of the tube forming is provided by an external pressurizing device. The internal pressure acts uniformly on the inner surface of the pipe member. In addition to its function of bulging [40], the pressure also prevents the inner part from bending and folding and produces an ultra-high-pressure hydrostatic stress. The pressing force is provided by the left and right pressing punches. The squeezing force mainly shifts the metal to the deformed rounded transition zone, which is beneficial to the flow of the metal, so as to continuously replenish the metal in the deformation process of the pipe, the balance punch provides the balance force of the end of the branch pipe, and its function is to counter balance of the liquid pressure inside the pipe on the top of the branch pipe, improve the stress and strain state of the branch pipe and the rounded transition zone, flatten the top of the branch pipe [41], and make it in the state of

compressive stress, therefore this finally becomes the force transmission zone. The combined action of these three forces allows the tube blank to be formed under ultra-high-pressure hydrostatic pressure [42].

2. Dies

(1) The shape and size of the die cavity, especially the radius of the corner radius of the transition zone, will directly determine the deformation of the tube blank.

(2) The manufacturing and assembly precision of the die is often neglected in the quantitative analysis for the asymmetry and eccentric part forming process. This is one of the key causes for the large deviation between the theoretical analysis and the test results.

(3) The surface quality of the die mainly refers to the surface roughness. This will greatly affect the friction coefficient.

(4) The rigidity and strength of the die directly affect the geometry and dimensional accuracy of the part.

In addition, since the liquid is a bulging medium [43], the precision of the die greatly affects the sealing of the high-pressure liquid and determines whether the forming can proceed. Therefore, in the case of technical and economical rationality, the precision of die processing should be as high as possible, and the rigidity should be as great as possible.

3. Extrusion Punch

This mainly refers to the accuracy of the synchronous movement of the two left and right extrusion punches in hydroforming. The synchronism of the punch movement affects the symmetry of the deformation and has a strong influence on the deformation size. If the punch movement cannot be kept in sync, large shear deformation will occur in the transition zone, which is very unfavorable for the process [44]. Therefore, effective measures should be taken to ensure the accuracy of synchronous motion.

4. Lubrication

Friction can cause uneven distribution of stress and strain fields and increase of deformation resistance, plus scratches on the surface of the workpiece. Therefore, a suitable lubricant (the hydraulic liquid and oil are used often) should be used, and a good lubrication state should be maintained to reduce friction.

Chapter 3 FEA Simulation Software Tools

3.1 Finite Element Analysis

The Finite Element Method is one of the most widely used and most viable methods in numerical analysis of metal forming [45]. In the past two decades, automotive parts manufacturers have done a lot of research on finite element theory, unit type, constitutive material relationship, model contacting and algorithm, which makes its application in metal forming analysis become increasingly more common. From the 1970s to the mid-to-late 1980s, researchers could only solve the plane and the axisymmetric problem. However, by the 1990s, more complicated three-dimensional problem could be solved [45]. At present, people are constantly improving the calculation efficiency and precision, and beginning to develop in the direction of practical use.

The basic principle of the finite element method is to divide the continuous medium to solve the unknown field variable into a finite number of units [46], which are connected by nodes. The field variables in each unit are determined by the node value through the interpolation function, and the force between the units is transferred by the nodes, which is based on the equation of motion or stiffness equation established by the principle of virtual work or similarly the variational principle of energy functionals. Then the elements are integrated to form the overall motion equation or the overall stiffness equation of the problem. Finally, the numerical solution is performed to obtain the node

value of the basic unknown (generally displacement), and then the values of other field variables are obtained.

At present, the finite element method has become one of the main numerical analysis methods for analyzing and studying metal plasticity problems. Compared with other methods, the finite element method has a lot of advantages. First of all, due to the flexibility of the unit shape [47], the finite element method can be applied to any material model, any boundary condition, and any structural shape. Hence various plastic forming processes of metal materials can be analyzed by the finite element method. Secondly, the finite element method can better deal with problems such as frictional contact boundaries; these cannot be compared with other methods. Thirdly, the finite element method can provide detailed information on the metal plastic forming process, including stress field and strain field, velocity field, equivalent strain distribution, etc [48]. Moreover, the finite element method can be combined with computer-aided design technology to provide a reliable basis for designing the forming process and die structure design. Lastly, because the calculation process is completely computerized, it can solve the forming problem of large and complex fragments.

However, the finite element method also has its limitations. Firstly, the finite element method cannot analyze the forming problem that is completely determined after the numerical expression of the process conditions, and only the discrete numerical solution

can be obtained. The influence of each process factor on the process and the relationship between them are not easy to uncover, so multiple calculations need to be performed for the comparative analysis [49]. Secondly, the amount of calculation is large when performing large plastic deformation, so a large-capacity computer and a long calculation time are required. Thirdly, the calculation accuracy. Since the finite element method is a numerical calculation method, there are various factors that cause errors in a calculation process, such as the minor differences between a numerical model and a real model, boundary contact condition processing and iterative convergence processing. These deficiencies [50] are constantly being improved with the further improvement of finite element theory and the rapid advancement of computer technology.

3.2 DYNAFORM for Metal Forming

The finite element technology has been produced and put into use for 30 years, and the rapid development of computer technology and the improvement of computing methods have greatly promoted the development and application of finite element technology. At present, the finite element analysis software tools, such as eta/DYNAFORM, ABAQUS, CATIA, etc. [25], are widely used in the field of metal plastic forming analysis. By analyzing and comparing the characteristics and application of each finite element simulation software, aiming at the hydraulic forming deformation characteristics of the

pipe fittings, the eta/DYNAFORM software was used to simulate the hydraulic forming process of the pipe.

Eta/DYNAFORM is a special software tool for metal forming simulation. It is a special software package developed by ETA (Engineering Technology Associates) for metal forming simulation, which can help die designers to significantly reduce the die development design time and test cycle, not only does it have good ease of use, but it also includes A large number of intelligent automatic tools that can easily solve various types of plate forming problems. Its main application areas are: 1. typical sheet metal forming process such as stamping, blanking, drawing, bending, rebounding, and multi-step forming; 2. hydroforming, roll forming; 3. die design; 4. press load analysis and so on.

It can help engineers and technicians reduce the stamping product development cycle, solve the problems of formability, wrinkling, rebounding, indentation and press tonnage prediction in die design. It is an efficient metal forming simulation tool. Compared with other finite element analysis software tools, DYNAFORM has the advantages of accurate simulation results, single environment analysis, automation, display solution method, implicit solution method, and seamless conversion.

DYNAFORM includes all the functions of interface, pre- and post-processing, and analytical solutions required for board forming analysis. It can predict the cracking,

wrinkling, thinning, scratching and rebound of the sheet during the forming process, and evaluate the forming properties of the sheet, thus helping the sheet forming process and die design. Currently, eta/DYNAFORM has been widely used in major automobile, aviation, steel companies, and many universities and research institutes.

3.3 Main Features of DYNAFORM

The DYNAFORM finite element analysis system is a metal forming simulation software package based on LS-DYNA [51]. Its solver LS-DYNA is the world's most well-known finite element explicit nonlinear dynamic analysis solver. It has a very powerful calculation function thus it is widely used. The main features of DYNAFORM finite element analysis software are: 1. integrated operating environment, no data conversion: complete pre- and post-processing functions, no text editing operation, all operations are performed under the same interface; 2. Solver: Using the industry-famous and most powerful LS-DYNA, it is the founder and leader of dynamic nonlinear display analysis technology, solving the most complex metal forming problems; 3. Process analysis process: Covers many factors affecting the stamping process; has a good process interface, easy to learn and use; 4. solidified practical engineering experience for a variety of platforms. [52]

Chapter 4 Methodology

4.1 Torsion Beam Finite Element Model

As shown in Figures 8, it shows the mesh model in the finite element simulation analysis of the torsion beam tube hydroforming in DYNAFORM. The torsion beam is a face-symmetric geometry, its symmetry plane is the face formed by the main axis and the branch pipe axis.

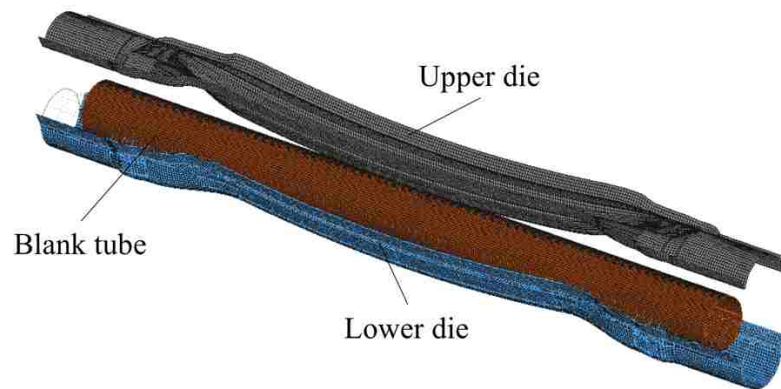


Figure 8. FEA model in DYNAFORM.

4.2 Torsion Beam Material

At the request of the customer, CP800 was selected as the simulation material. CP800 is a high-strength steel, and its stress-strain curve (Figure 9) is available in the material bank of DYNAFORM. The yield strength of CP800 is 778 MPa [53].

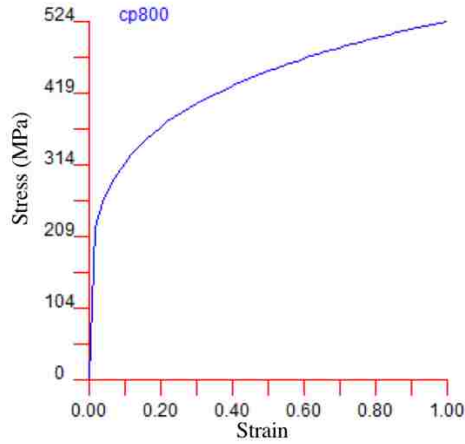


Figure 9. CP800 stress-strain curve.

Following the cylinder vessels yield strength formulas [54]

$$\sigma = \frac{pr}{t}$$

Equation Variables
σ =the yield strength (MPa)
p =the pressure (MPa)
r =the radius (mm)
t =thickness (mm)

Table 1. Equation variables.

The maximum pressure can be obtained as $p_{max} = \sigma \frac{t}{r}$, where σ stands for the yield strength of CP800 is 778 MPa. Moreover, this maximum pressure cannot be exceeded when the die is closed as well, nor when the entire exterior surface of the part is in contact with the press die tooling. The thickness is 3.5 mm and the diameter of the tube is

101 mm (Figure 5, Section 1.3), so the radius comes to 50.5 mm. Thus, after implementing all the numbers, p_{max} becomes,

$$p_{max} = 778 \text{ MPa} \frac{3.5 \text{ mm}}{50.5 \text{ mm}}$$
$$p_{max} = 53.9 \text{ MPa}$$

This means the tube with thickness 3.5 mm and the material CP800, can only bear the pressure value less than 53.9 MPa, otherwise it has a highly increased possibility of breaking, and so the setting of the pressure during simulation cannot exceed 53.9 MPa.

4.3 Simulation Factors

Design requirement #6 of the technical requirements asserts that the thinning rate should not exceed 10% (Figure 6). This is crucial because it is the determining condition as to whether the results can be considered valid. The thinning rate needs to be calculated after each simulation, and if the thinning rate is more than 10%, the simulation will be considered unacceptable because the metal thickness cannot be less than 90% of the original cross-sectional thickness. Thus, if the thinning rate exceeds 10%, the metal thickness will be considered inadequate. As outline Table 2, there are three factors that should be considered during this simulation: the pressure, the mesh size, and the loading time.

Factors		
Pressure (MPa)	Mesh (mm)	Time (s)
0	5	1
		2
		3
	10	1
		2
		3
	15	1
		2
		3
10	5	1
		2
		3
	10	1
		2
		3
	15	1
		2
		3
20	5	1
		2
		3
	10	1
		2
		3
	15	1
		2
		3
30	5	1
		2
		3
	10	1
		2

Factors		
Pressure (MPa)	Mesh (mm)	Time (s)
	15	3
		1
		2
		3
40	5	1
		2
		3
	10	1
		2
		3
	15	1
		2
		3
50	5	1
		2
		3
	10	1
		2
		3
	15	1
		2
		3

Table 2. Three factors with different levels.

The initial pressure has six levels, which are 0, 10 MPa, 20 MPa, 30 MPa, 40 MPa and 50 MPa (Table 2). High pressure may result in breaking of components because the maximum pressure that the material can bear is 53.9 MPa (Section 4.2), so the greatest pressure setting is 50 MPa. The pressure value here is the initial pressure before the hydroforming process gets started. For example, when the pressure is at 0, that does not

mean the whole process has zero pressure, but the initial pressure is at 0, so the pressure factor is the initial pressure, not the increasing pressure during the process. The hydraulic liquid, as the use of lubricant, will be infused before the whole process gets started. Once it is done, the axial feedings at both sides will start to move close to the tube ends, in order to seal the tube prior to the stamp cycle (Figure 10).

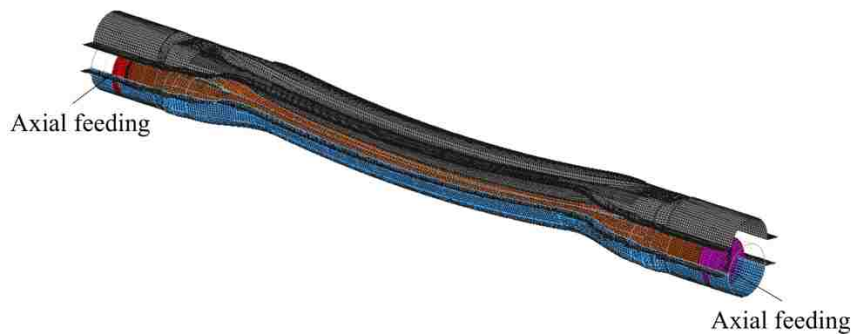


Figure 10. Tube sealing prior to stamp cycle.

The pressure will be increasing due to the upper die started to form the tube, and the hydraulic liquid inside will counter-act on the inner surface of the tube, which is how the pressure created, and this high pressure would be released prior to opening the die. Thus, the increasing pressure during the stamping cycle is various, and DYNAFORM simulations also provide the pressure increase during the stamp cycle.

Secondly, the mesh size will affect the calculation time and results during the FEA simulation. Smaller mesh sizes will give more precise simulation results, but it takes

more time, so the mesh size has been determined as three levels, which are 5 mm, 10 mm and 15 mm.

The third factor, loading time (formation cycle time), also has three levels: 1, 2, and 3 seconds. The time mimics the duration of the actual manufacturing process. This is the time duration that the upper die requires to finish the job starting from tube contact to form completion. For example, when the time is at one second, the time between surface contact with the tube to the tube becoming the desired shape of a torsion beam is one second. The time is very important because different time setting will affect the thinning rate in the end. According to the simulation results in Chapter 5, the faster the time setting is, it is more possible to have a breakage at the tube.

Chapter 5 Results

5.1 Simulation Results

The three factors with different levels have been tested one by one during separate simulations in DYNAFORM. There were 54 simulations in total, and the thinning rates have been calculated and shown in the fifth column of Table 3. The Note (Table 3) was made to indicate whether the thinning rate was greater or smaller than 10%. However, there were some warning messages reported by DYNAFORM due to some issues, such as some parts of the pipe edging were broken (minor little breakage at certain points on the surface of the torsion beam) by the end of the simulation. Although the determining condition of success is the thinning rate being less than 10%, some thinning rates with less than 10% were still recorded as warnings by DYNAFORM, and the most common warning situation would be that the pressure was set too high. Ultimately the project (pipe) experienced cracking whilst using these settings. Although the internal hydraulic pressure was released prior to opening the die, this would not resolve concern of the pressure being too high since the breakage occurred during the forming.

Runs	Pressure (MPa)	Mesh (mm)	Time (s)	Thinning Rate (%)	Note
1	0	5	1	23.367	>10%
2			2	1.694	Warning
3			3	4.405	<10%
4		10	1	4.642	<10%
5			2	0.575	Warning
6			3	1.742	Warning
7		15	1	14.242	>10%

Runs	Pressure (MPa)	Mesh (mm)	Time (s)	Thinning Rate (%)	Note
8			2	2.678	Warning
9			3	11.942	Warning
10			1	15.38	>10%
11	10	5	2	2.198	Warning
12			3	2.326	Warning
13			1	28.262	>10%
14		10	2	30.255	>10%
15			3	27.488	>10%
16			1	26.743	>10%
17		15	2	18.61	>10%
18			3	25.638	>10%
19			1	15.288	>10%
20	20	5	2	3.088	Warning
21			3	20.359	Warning
22			1	115.121	Warning
23		10	2	100.05	Warning
24			3	104.575	Warning
25			1	2956	Warning
26		15	2	189.888	Warning
27			3	100	Warning
28			1	16.58	>10%
29	30	5	2	4.965	Warning
30			3	4.695	Warning
31			1	102.396	Warning
32		10	2	100.179	Warning
33			3	100.316	Warning
34			1	101.546	Warning
35		15	2	101.584	Warning
36			3	101.923	Warning
37			1	18.145	>10%
38	40	5	2	7.119	Warning
39			3	118.937	Warning
40			1	102.942	Warning
41		10	2	101.477	Warning

Runs	Pressure (MPa)	Mesh (mm)	Time (s)	Thinning Rate (%)	Note
42	50	15	3	116.246	Warning
43			1	340.224	Warning
44			2	85.006	Warning
45			3	84.436	Warning
46	50	5	1	27.338	Warning
47			2	131.829	Warning
48			3	119.604	Warning
49		10	1	108.948	Warning
50			2	106.849	Warning
51			3	100.12	Warning
52		15	1	99.983	Warning
53			2	100.192	Warning
54			3	94.254	Warning

Table 3. DYNAFORM simulation results.

According to Table 3, the greater the pressure set, the more warnings were reported. When pressure was at 10 MPa, 20 MPa and 30 MPa, there was only one calculation without any warning message for each pressure setting. As for the 50 MPa pressure setting, all nine simulations had warning messages, no matter what the mesh or time settings were. Overall, only two settings can be considered as acceptable, which are run 3 and 4, because they both had no warning message reported and the thinning rates were less than 10%. Since the objective is to minimize the thinning rate, the best result was from run 3 with a 4.4% thinning rate (Table 3). When the thinning rate was greater than 100%, there was a warning message from DYNAFORM, which meant there was a breakage to the tube. For example, a four-digit number (2956) appears in the thinning rate

column of Table 3, which is a theoretical result generated by DYNAFORM and indicates the breakage of the tube.

5.2 Mathematical Model

In order to create a reference equation for future thinning rate predictions under the similar manufacturing processes, a regression equation was generated with MNITAB. Thus, instead of running the FEA simulation again, the thinning rate can be calculated using this equation.

The worksheet input is shown in Table 4. There were two factors had been considered in MINITAB analyzing, which were pressure and time. Only pressure and time would affect the manufacturing processes, and the mesh size is only related to the FEA simulation. Since the regression equation will be used to predict the thinning rate by manufactures, the mesh size will not be considered for the regression equation. The time has three levels as the FEA simulation, but the pressure has five levels instead of six because the values of thinning rates with pressure at 50 were unacceptable and also warning messages were reported in DYNAFORM, so those values have been removed in order to approve the accuracy of the regression equation. All the thinning rates from DYNAFORM have been written down. Although when the thinning rates are greater than 10% is not acceptable by

the manufactures, they are still the real results from the FEA simulations, and still need to be analyzed for research.

StdOrder	RunOrder	PtType	Blocks	P	T	thinning rate
1	1	1	1	0	1	4.642
2	2	1	1	0	2	0.575
3	3	1	1	0	3	1.742
4	4	1	1	10	1	28.262
5	5	1	1	10	2	30.255
6	6	1	1	10	3	27.488
7	7	1	1	20	1	115.121
8	8	1	1	20	2	100.05
9	9	1	1	20	3	104.575
10	10	1	1	30	1	102.396
11	11	1	1	30	2	100.179
12	12	1	1	30	3	100.316
13	13	1	1	40	1	102.942
14	14	1	1	40	2	101.477
15	15	1	1	40	3	116.246

Table 4. MINITAB worksheet.

During the analysis, there was no replicated simulation (n=1) because the data was collected from software tool would produce the same results for the thinning rates. The obtained results were irrespective of the number of times the simulations were run but were only identical as long as the values of the input variables were the same. Thus, there was no need to produce further repeats for the simulations.

The regression equation is obtained as

$$\text{thinning rate} = 13.4 + 2.814 P - 0.30 T$$

where P stands for pressure and T is for time. This equation can predict similar simulation scenarios in the future. This equation can be used to predict theoretical results by inputting the values of the variables (pressure and time) in the current simulation. For example, if we want to know the thinning rate with the pressure at 2 MPa and time at 1 second, there is no need to run the FEA simulation in DYNAFORM when we have this equation. Simply implement the numbers, the theoretical thinning rate is calculated as

$$\text{thinning rate} = 13.4 + 2.814*2 - 0.3*1 = 18.728$$

5.3 Significant Factors

Based on the evidence provided by the data sample, hypothesis testing is a rule to specify whether a statement is affirmative or negative. The P-value (the probability) is commonly used in hypothesis testing, and it reflects the probability of an event occurring. The P-value is type I error, which is the probability of rejecting H_0 when H_0 is true. Whilst analysing the data in MINITAB, the most significant factor can be determined according to the P-value. The P-value is a way of determining whether the test factors were rejected or not at a given level of significance [55]. The P-value obtained by the statistical method according to the significance test was generally considered the data to be significant at $P < 0.05$, so it is customary to define the level of significance to be 0.05 [55]. When

$P > 0.05$, the factor is not significant. According to the statistical principle, the null hypothesis could not be denied, but the null hypothesis was not established. In this analysis, if the P-values of factors are greater than 0.05, it does not mean that the two factors are not significant or equivalent, there are more analysis need to be done to determine the significance of factors. The P-values can be obtained from Table 5 (ANOVA, the analysis of variance table) which is generated by MINITAB.

Source	DF	Adj SS	Adj MS	F-Value	P-Value
Regression	2	23762.2	11881.1	22.51	0.000
P	1	23761.3	23761.3	45.02	0.000
T	1	0.9	0.9	0.00	0.968
Error	12	6333.2	527.8		
Total	14	30095.4			

Table 5. ANOVA (analysis of variance).

By observing the P-value, the factor pressure is 0, which can be considered as significant. However, the P-value of time is 0.968, which is way greater than 0.05, so it does not affect the results too much. In order to confirm the significance furthermore, the individual source effects can be directly compared by calculating and ranking the percentage contribution of sum of squares. The calculations of the percentage of contribution of Adj SS are shown in Table 6.

Source	Calculation	Percentage Contribution
Pressure	$\frac{23761.3}{30095.4}$	78.9%
Time	$\frac{0.9}{30095.4}$	0.1%
Error	$\frac{6333.2}{30095.4}$	21.0%
Total		1

Table 6. Percentage contribution of sum of square.

Observing the calculation results (Table 6), we find that the greatest percentage contribution is the pressure at 78.9%, and this result match with the conclusion based on the P-value. Thus, we confirm that pressure is a significant factor.

5.4 Model Summary

In general, according to the value of R-sq (R-squared) in Table 7, we can say that the model fits with the data. The value of R-sq is between 0 to 100%, and it represents the percentage of variation in the results of the experiments. The higher the R-sq value (closer to 100%), the better the model fits the data [56]. In the model summary, the R-sq is 78.96% (Table 7), which is very close to 80%, thus the model is adequate.

As we can see in Table 7, the R-sq(adj) (adjusted R-squared) is a little smaller than R-sq, 75.45%. R-sq(adj) is used to compare with different predictors. The predictors here are the pressure and time, but if more predictors are added to the model, the R-sq will increase even if the model does not actually improve [56]. The adjusted R-sq value contains the number of predictors in the model to in order to choose the right model. As for R-sq(pred), 68.7%, it is the predicted R-sq, and is used to predict the response of new observations, and the model with greater R-sq(pred) typically has better predictive capability [56].

S	R-sq	R-sq(adj)	R-sq(pred)
22.9732	78.96%	75.45%	68.70%

Table 7. Model Summary.

5.5 Scatterplots

By plotting the regression line and the values of factors separately, Figure 11 and Figure 12 are obtained. Figure 11 shows the regression line with the scatter plots of pressure values, while Figure 12 shows the regression line with the time values. These figures illustrate that the pressure plays a major role in the regression equation, but the time does not substantially affect the equation. These are the same results as in the P-value in the ANOVA table, as well as matching the percentage contribution of sums of squares. Thus, we can say that pressure is significant to the model and also sensitive to the simulation results, which explains the reason that the FEA simulation started to suggest breakage at the tube when the pressure was set too high.

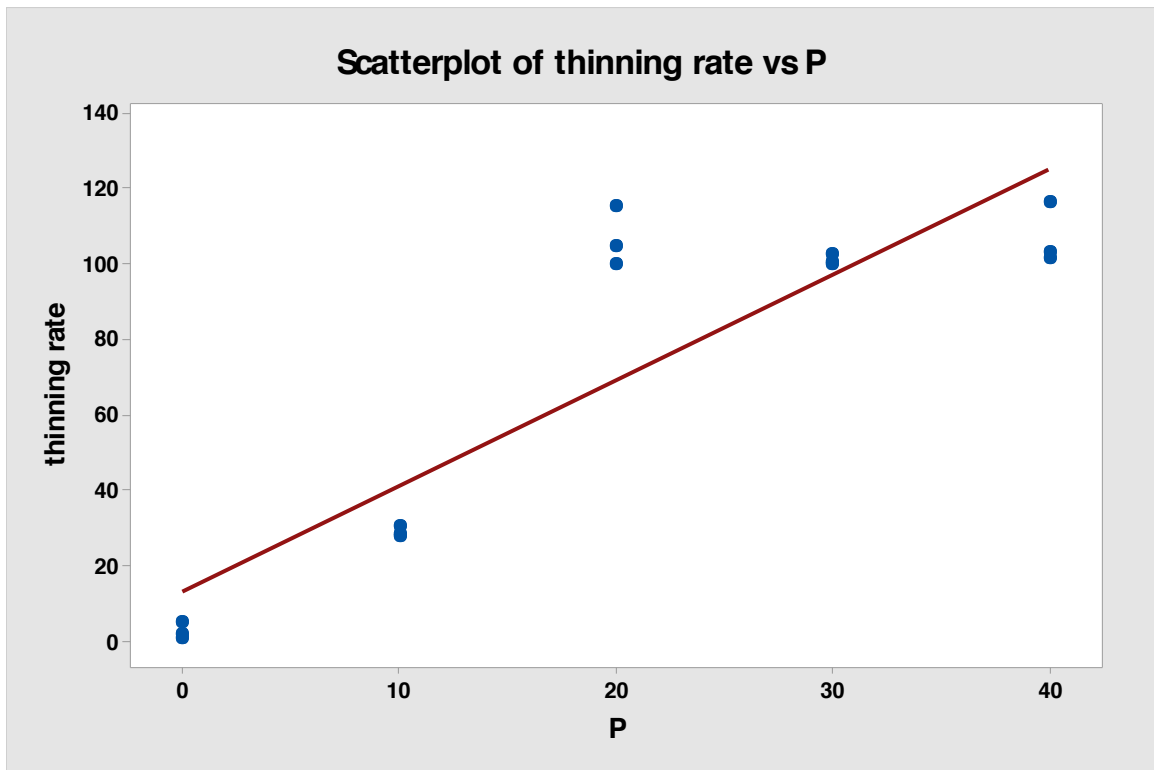


Figure 11. Scatterplot of thinning rate vs P.

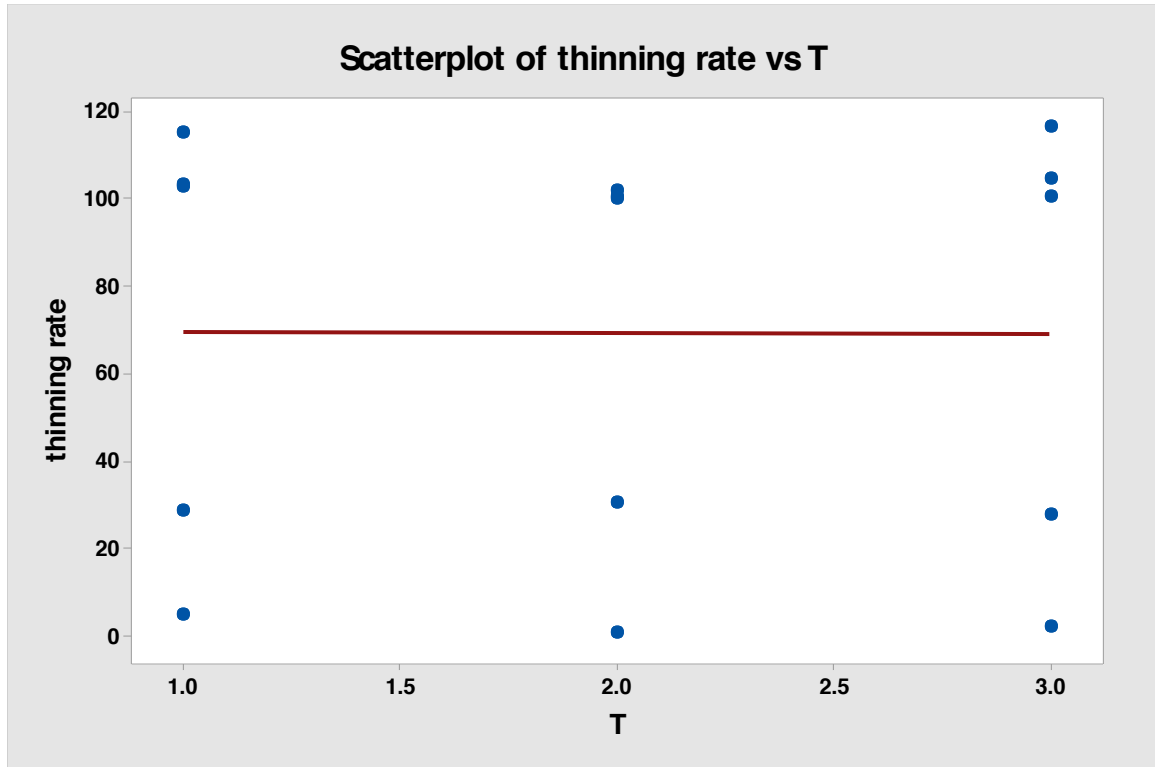


Figure 12. Surface plot of thinning rate vs T.

The 3D scatterplots were also obtained in order to see the results more clearly. T (time) and P (pressure) are the predictors in this analysis, and the thinning rate is the response variable, which is represented by a surface of the 3D surface plot in Figure 13. Because the purpose is to minimize the thinning rate, the surface (Figure 13) illustrates that the pressure should be set as low as possible, which corresponds to the lowest thinning rate with the pressure at 0. Moreover, the time settings seem to give very close results to this 3D scatter plot. For example, when we look at the lowest thinning rate, the corresponding time is at 1s, 2s or 3s. This matches the result that the factor, time, is not significant to the mathematic model or the simulation results. Figure 14 is the 3D scatter plot that

represents the same results as Figure 14, but the scattered dots are more obvious to demonstrate their locations in the 3D coordinates and obtain the values.

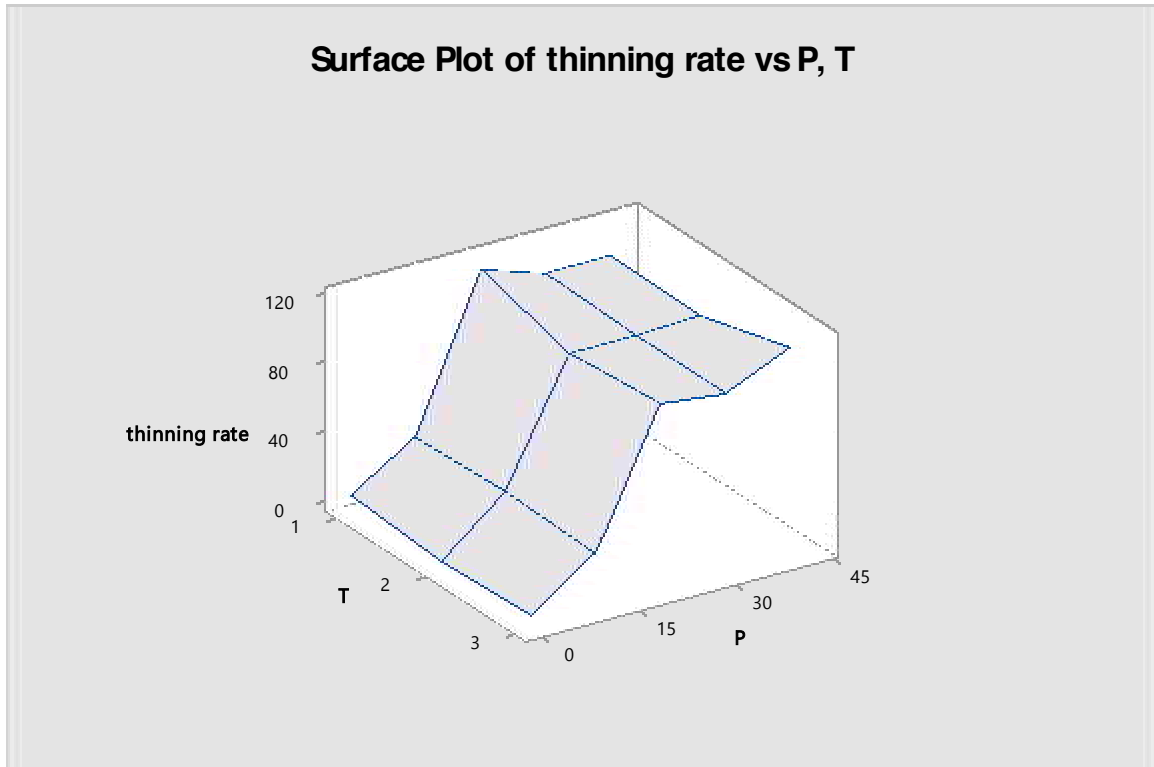


Figure 13. Surface plot of thinning rate vs P, T.

3D Scatterplot of thinning rate vs P vs T

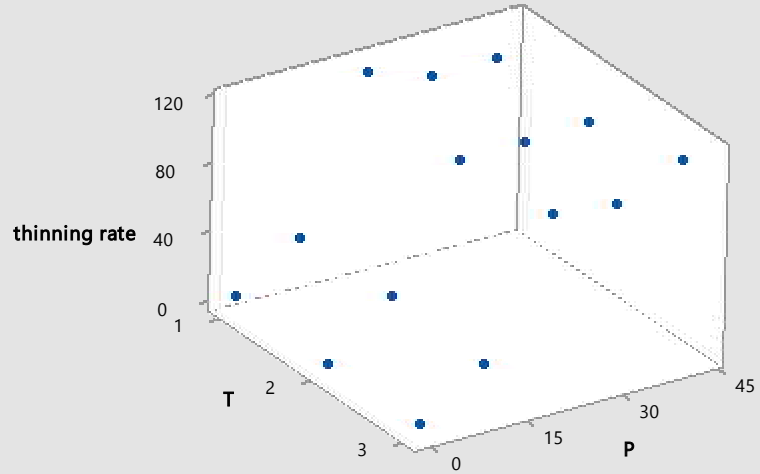


Figure 14. 3D scatterplot of thinning rate vs P vs T.

Chapter 6 Conclusions and Future Research

6.1 Conclusions

The current study analyzed 54 combinations of the different factor settings—pressure, mesh size, and time—for the simulation of the torsion beam tube hydroforming process, and the simulations were run one by one in DYNAFORM. The final thinning rates of each simulation were obtained and the lowest thinning rate (4.4%) was selected with the pressure at 0 MPa, mesh at 5 mm and time at 3 seconds. Pressure is clearly the significant factor for the thinning rates, but time had little effect on the thinning rates. It was determined that the maximum theoretical pressure that CP800 can bear is 53.9 MPa. During this tube hydroforming process, high pressure greater than 10 MPa may result in unacceptable issues such as component breakage.

The model is adequate, and the methods used in this thesis are both useful and beneficial. The model has been used in the manufacturing process already and can be applied repeatedly in future applications. Based on the collected simulation data in MINITAB a regression equation was created. This provided a reference equation that predicts the thinning rates by implementing the factors as desired, which in turn provides theoretical result more quickly than running a FEA simulation with new values of variables.

According to the data analysis results (P-value, Table 5, and the percentage contribution

of the adjusted sums of squares from the Analysis of Variance, Table 6), the significant factor (pressure) for this simulation has been determined.

6.2 Future Research

The current study has demonstrated that this model is applicable to the tubes with shapes and dimensions consistent with the material selected for the study, and it is reasonable to assume that can be applied in similar circumstances. However, this needs to be verified by future research. Thus, to confirm these findings and determine their broader applicability, future researchers should simulate the same study with the similar but varied factors and scenarios, including different sizing, materials, and the parameters of the models. Introducing these kinds of conditional changes has the potential to determine this model's full range of applications. The physical measurements of actual production parts are also recommended, in order to validate the accuracy of the simulation results and the regression equation.

Based on the analysis, pressure factor will need the most consideration before undertaking real world forming projects in the future. During this experiment the pressure was tested at six levels, and 54 simulations were run. Therefore, the research still has some limitations. In order to make the results more precise, more detailed pressure

settings should be added and to be analyzed in the future. For example, adding four more levels with 2 MPa, 4 MPa, 6 MPa and 8 MPa to be simulated in DYNAFORM.

Improving accuracy could give enhance pressure setting, which will benefit the hydroforming process.

Reference

1. Huétink, J., Lugt, J. V., & Vreede, P. T. (1988). A Mixed Eulerian-Lagrangian Finite Element Method For Simulation Of Thermo-Mechanical Forming Processes. *Modelling of Metal Forming Processes*, 57-64. doi:10.1007/978-94-009-1411-7_7
2. Dohmann, F., & Hartl, C. (1996). Hydroforming - a method to manufacture light-weight parts. *Journal of Materials Processing Technology*, 60(1-4), 669-676. doi:10.1016/0924-0136(96)02403-x
3. Shirayori, A., Fuchizawa, S., & Narazaki, M. (2007). Influence of axial feeding on the growth of circumferential thickness deviation in free hydraulic bulging. *Metals and Materials International*, 13(2), 185-189. doi:10.1007/bf03027571
4. Manufacturing Technology for Aerospace Structural Materials. (2006). doi:10.1016/b978-1-85617-495-4.x5000-8
5. Design of Prestressed Concrete Beams Subjected to Combined Bending, Shear, and Torsion. (1975). *ACI Journal Proceedings*, 72(3). doi:10.14359/11117
6. Herakovich, C. T. (2016). Mechanics of Solids. *A Concise Introduction to Elastic Solids*, 1-7. doi:10.1007/978-3-319-45602-7_1
7. Aoyama, Y., Kawabata, K., Hasegawa, S., Kobari, Y., Sato, M., & Tsuruta, E. (1990). Development of the Full Active Suspension by Nissan. *SAE Technical Paper Series*. doi:10.4271/901747
8. Wang, E., Ying, L., Wang, W., Rakheja, S., & Su, C. (2007). Analyses of Inverse Model Based Semi-Active Control of Vehicle Suspension with Magneto-Rheological Dampers. *2007 IEEE International Conference on Control Applications*. doi:10.1109/cca.2007.4389234
9. Fujita, M., Matsumura, F., & Uchida, K. (1990). Experiments on the H/sup infinity / disturbance attenuation control of a magnetic suspension system. *29th IEEE Conference on Decision and Control*. doi:10.1109/cdc.1990.203283
10. Qiu, X. G., & Huang, Y. D. (2012). Study on Numerical Simulation of Automobile Covering Parts Stamping Forming Process. *Applied Mechanics and Materials*, 271-272, 509-514. doi:10.4028/www.scientific.net/amm.271-272.509
11. Alaswad, A., Benyounis, K., & Olabi, A. (2012). Tube hydroforming process: A reference guide. *Materials & Design*, 33, 328-339. doi:10.1016/j.matdes.2011.07.052
12. Kleiner, M., Geiger, M., & Klaus, A. (2003). Manufacturing of Lightweight Components by Metal Forming. *CIRP Annals*, 52(2), 521-542. doi:10.1016/s0007-8506(07)60202-9
13. Allwood, J., & Utsunomiya, H. (2006). A survey of flexible forming processes in Japan. *International Journal of Machine Tools and Manufacture*, 46(15), 1939-1960. doi:10.1016/j.ijmachtools.2006.01.034
14. Proceedings of the FISITA 2012 World Automotive Congress. (2013). *Lecture Notes in Electrical Engineering*. doi:10.1007/978-3-642-33741-3
15. Koç, M., & Altan, T. (2001). An overall review of the tube hydroforming (THF) technology. *Journal of Materials Processing Technology*, 108(3), 384-393. doi:10.1016/s0924-0136(00)00830-x

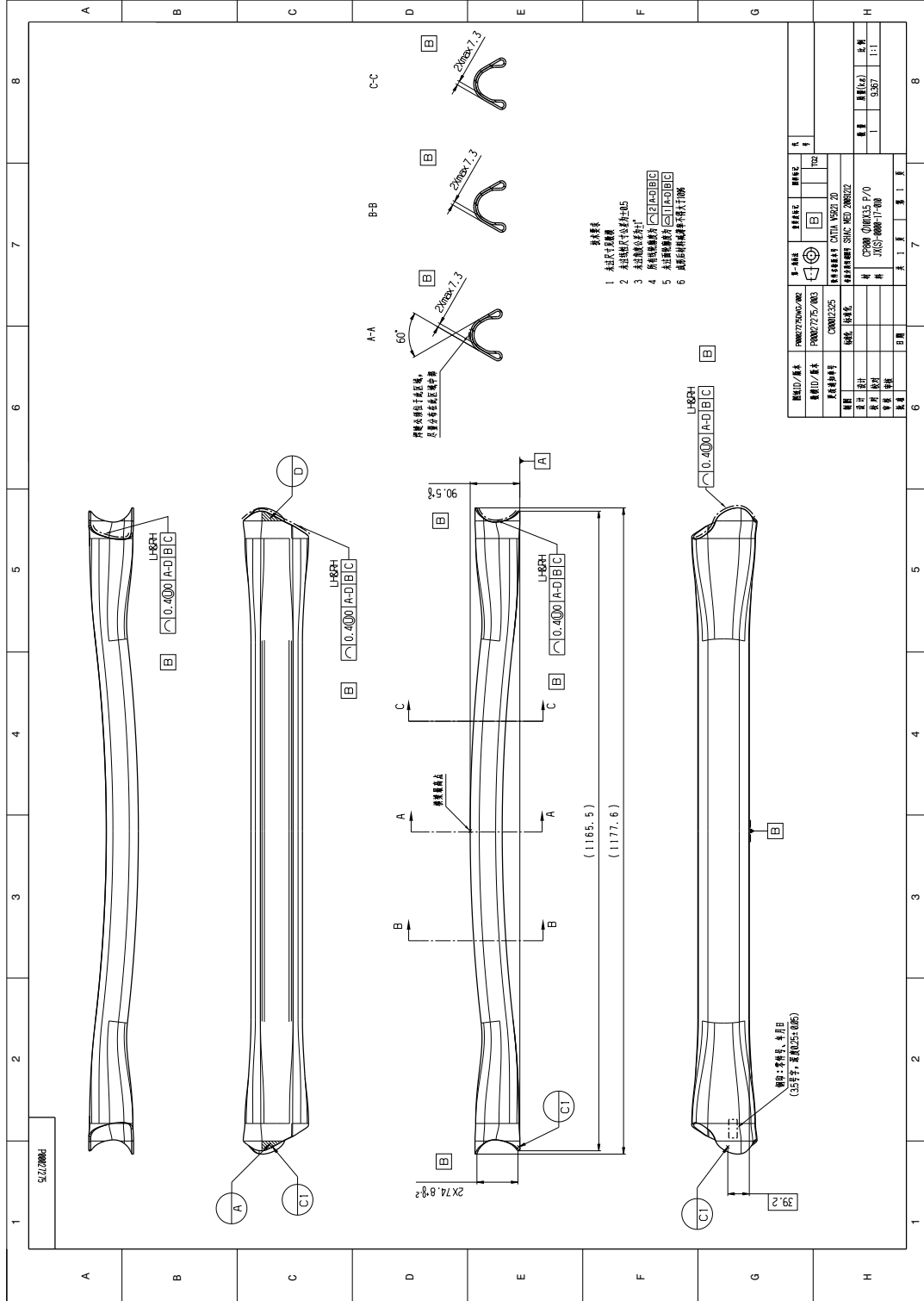
16. Imaninejad, M., Subhash, G., & Loukus, A. (2004). Experimental and numerical investigation of free-bulge formation during hydroforming of aluminum extrusions. *Journal of Materials Processing Technology*, 147(2), 247-254. doi:10.1016/j.jmatprotec.2004.01.004
17. Fuchizawa, S. (1987). Influence of Plastic Anisotropy on Deformation of Thin-walled Tubes in Bulge Forming. *Advanced Technology of Plasticity 1987*, 727-732. doi:10.1007/978-3-662-11046-1_6
18. Zhang, S., Wang, Z., Xu, Y., Wang, Z., & Zhou, L. (2004). Recent developments in sheet hydroforming technology. *Journal of Materials Processing Technology*, 151(1-3), 237-241. doi:10.1016/j.jmatprotec.2004.04.054
19. Ahmetoglu, M., & Altan, T. (1999). Tube Hydroforming - State-of-the-Art and Future Trends. *SAE Technical Paper Series*. doi:10.4271/1999-01-0675
20. Singh, H. (2003). *Fundamentals of hydroforming*. Dearborn, MI: Society of Manufacturing Engineers.
21. Paunoiu, V., Ciocan, O., & Nicoara, D. (2010). NUMERICAL STUDY OF TUBE HYDROFORMING TECHNOLOGY. *International Journal of Modern Manufacturing Technologies*, 2, 67-72.
22. Koç, M. (2008). *Hydroforming for advanced manufacturing*. Cambridge, UK: Woodhead.
23. Zhang, S. (1999). Developments in hydroforming. *Journal of Materials Processing Technology*, 91(1-3), 236-244. doi:10.1016/s0924-0136(98)00423-3
24. An, H. (2012). *Multi-objective optimization of tube hydroforming using hybrid global and local search*(Unpublished master's thesis).
25. Kaushal, A. (2004). *Vehicle front rail impact trigger: A new conceptual design, manufacturing and impact performance through FEA simulation*.
26. Kim, J., Kang, B. S., & Hwang, S. M. (2002). Preform design in hydroforming by the three-dimensional backward tracing scheme of the FEM. *Journal of Materials Processing Technology*, 130-131, 100-106. doi:10.1016/s0924-0136(02)00760-4
27. Zampaloni, M., Pourboghraat, F., Yankovich, S., Rodgers, B., Moore, J., Drzal, L., . . . Misra, M. (2007). Kenaf natural fiber reinforced polypropylene composites: A discussion on manufacturing problems and solutions. *Composites Part A: Applied Science and Manufacturing*, 38(6), 1569-1580. doi:10.1016/j.compositesa.2007.01.001
28. Hung, J., & Lin, C. (2012). Fabrication of micro-flow channels for metallic bipolar plates by a high-pressure hydroforming apparatus. *Journal of Power Sources*, 206, 179-184. doi:10.1016/j.jpowsour.2012.01.112
29. P. (1989). *Finite Element Method and It's Application of Forging Engineering*. Xi'an: Northwestern Polytechnical University Press.
30. Abedrabbo, N. (2004). Optimization of a Tube Hydroforming Process. *AIP Conference Proceedings*. doi:10.1063/1.1766687

31. Addis, A. K. (2018). Automobile Roof Panel Forming: Prediction and Compensation of Springback and Application of Numerical Simulation Based on Dynaform. *World Journal of Engineering and Technology*,06(04), 914-928. doi:10.4236/wjet.2018.64061
32. Kim, J., Chung, K., Lee, W., Kong, J., Ryu, H., Kim, D., . . . Chung, K. (2009). Optimization of boost condition and axial feeding on tube bending and hydro-forming process considering formability and spring-back. *Metals and Materials International*,15(5), 863-876. doi:10.1007/s12540-009-0863-9
33. Hwang, Y., Wang, K., & Kang, N. (2011). T-Shape Tube Hydroforming of Magnesium Alloys With Different Outlet Diameters. *Journal of Manufacturing Science and Engineering*,133(6), 061012. doi:10.1115/1.4004851
34. Long, A., Ge, R., Zhang, Y. S., & Wei, X. (2011). Numerical Simulation of B-Pillar's Hot Press Forming Process and its Shape Optimization. *Applied Mechanics and Materials*,138-139, 749-753. doi:10.4028/www.scientific.net/amm.138-139.749
35. Zhao, J., Zhao, X., Dong, C., Zhao, X., & Kang, S. (2018). Effect of bainitic transformation combined with hot forming on the microstructure and mechanical properties of bainite-martensite multiphase steel. *Materials Science and Engineering: A*,731, 102-106. doi:10.1016/j.msea.2018.05.111
36. *LIGHTWEIGHT TWIST BEAM FINAL REPORT*(Rep.). (n.d.). Southfield, MI: AISI Steel Market Development Institute.
37. Arjan, R., Andrew, B., Paul, B., & Chris, W. (2014). Advanced High Stretch-Flange Formability Steels for Chassis & Suspension Applications. *4th International Conference on Steels in Cars and Trucks*,15-19.
38. LIU Fang-hui,QIAN Xin-yuan, & ZHANG Jie (2001);Application of CAD/CAE/CAM technology in design of mould for plastics and manufacturing[J];*Die & Mould Industry*.
39. HAN, C., HE, J., & YUAN, S. (2016). Hydroforming of an Automotive Torsion Beam with 780 MPa Advanced High Strength Steel. *JOURNAL OF NETSHAPE FORMING ENGINEERING*.
40. Sato, M., & Hara, N. (2011). Welding consumables for 780 and 950 MPa class of high-strength steel. *Welding International*,25(9), 663-669. doi:10.1080/09507116.2010.527044
41. Nakata, N., & Militzer, M. (2005). Modelling of Microstructure Evolution during Hot Rolling of a 780 MPa High Strength Steel. *ISIJ International*,45(1), 82-90. doi:10.2355/isijinternational.45.82
42. TIAN, F. (2011). Design of Closed Extrusion Die with Halving Concave Die Locked by Support-boards. *JOURNAL OF NETSHAPE FORMING ENGINEERING*.
43. Lin, S., & Chen, F. (2010). Die Design and Axial Feeding in the Tube-Hydroforming Process. *ASME 2010 International Manufacturing Science and Engineering Conference, Volume 1*. doi:10.1115/msec2010-34113

44. HAN, C., ZHANG, W., YUAN, S., ZHAO, F., DING, Y., & CAO, W. (2011). The effect of perform shape on hydroforming of a torsion beam. *Materials Science & Technology*.
45. Waterman, P. (n.d.). Evolution of Analysis. Retrieved December 1, 2010, from <https://www.digitalengineering247.com/article/evolution-of-analysis/>
46. Jung-Ho, C., & Noboru, K. (1985). An analysis of metal forming processes using large deformation elastic-plastic formulations. *Computer Methods in Applied Mechanics and Engineering*,49(1), 71-108. doi:10.1016/0045-7825(85)90051-9
47. Im, Y., & Kobayashi, S. (1985). Finite-Element Analysis Of Plastic Deformation Of Porous Materials. *Metal Forming and Impact Mechanics*,103-122. doi:10.1016/b978-0-08-031679-6.50014-x
48. Finite Element Modeling of Metal Forming Processes Using Updated Lagrangian Formulation. (n.d.). *Engineering Materials and Processes Modeling of Metal Forming and Machining Processes*,345-423. doi:10.1007/978-1-84800-189-3_6
49. Gronostajski, Z., & Hawryluk, M. (2007). Analysis of metal forming processes by using physical modeling and new plastic similarity condition. *AIP Conference Proceedings*. doi:10.1063/1.2729580
50. Lee, E. H., Mallett, R. L., & Mcmeeking, R. M. (1979). Stress and Deformation Analysis of Metal-Forming Processes. *Metal Forming Plasticity*,177-189. doi:10.1007/978-3-642-81355-9_11
51. Li, K. (2003, January). DYNA MORE. Retrieved from <https://www.dynamore.de/en/products/form>
52. KeisaAdministrator. (n.d.). DYNAFORM. Retrieved from <https://www.eta.com/inventium/dynaform>
53. Liu, Z., Lang, L., Ruan, S., Zhang, M., Lv, F., & Qi, J. (2019). Effect of internal pressure assisted on hydroforming for CP800 high-strength steel torsion beam. *Journal of the Brazilian Society of Mechanical Sciences and Engineering*,41(2). doi:10.1007/s40430-019-1570-9
54. Hibbeler, R. C., & Yap, K. B. (2014). *Mechanics of Materials*. Harlow: Pearson.
55. C., M. D. (2009). *Design and analysis of experiments*. Hoboken: John Wiler & Sons.
56. Interpret all statistics and graphs for Two-way ANOVA. (n.d.). Retrieved from <https://support.minitab.com/en-us/minitab-express/1/help-and-how-to/modeling-statistics/anova/how-to/two-way-anova/interpret-the-results/all-statistics-and-graphs/#s>

Appendices

Appendix A Technical requirements of the torsion beam



Appendix B Regression Analysis

USING.

Regression Analysis: thinning rate versus P, T
Analysis of Variance

Source	DF	Adj SS	Adj MS	F-Value	P-Value
Regression	2	23762.2	11881.1	22.51	0.000
P	1	23761.3	23761.3	45.02	0.000
T	1	0.9	0.9	0.00	0.968
Error	12	6333.2	527.8		
Total	14	30095.4			

pressure

Model Summary

S	R-sq	R-sq(adj)	R-sq(pred)
22.9732	78.96%	75.45%	68.70%

prediction

Coefficients

Term	Coef	SE Coef	T-Value	P-Value	VIF
Constant	13.4	17.8	0.75	0.466	
P	2.814	0.419	6.71	0.000	1.00
T	-0.30	7.26	-0.04	0.968	1.00

Regression Equation

thinning rate = 13.4 + 2.814 P - 0.30 T



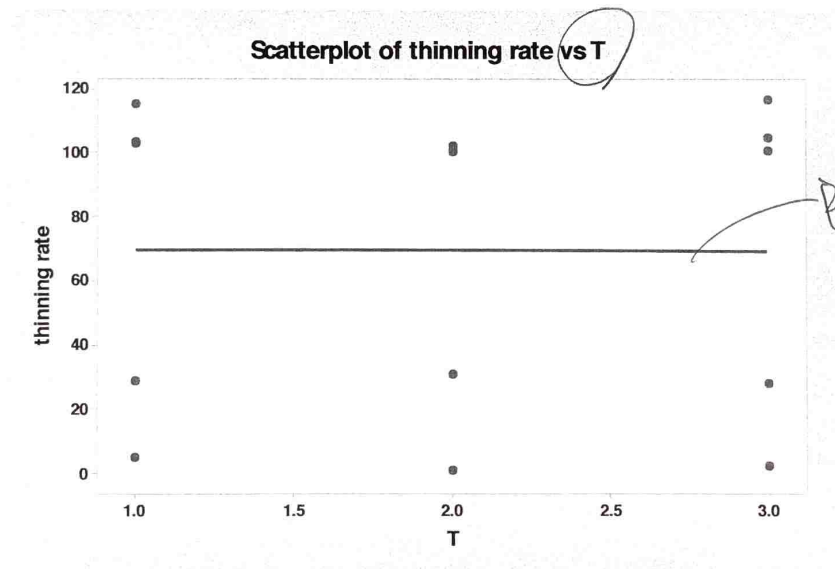
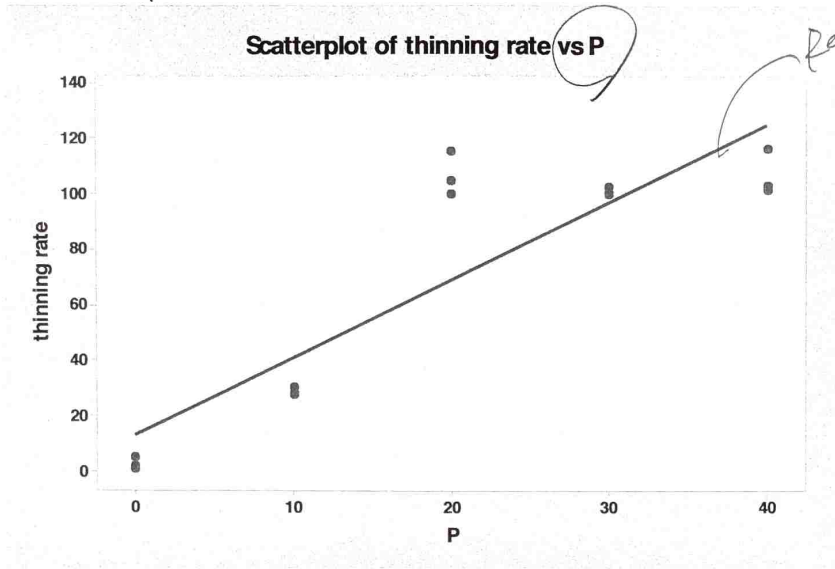
Fits and Diagnostics for Unusual Observations

Obs	thinning rate	Fit	Resid	Std Resid
7	115.12	69.38	45.74	2.18 R

R Large residual

Appendix C Regression Analysis – Regression Plots 2D

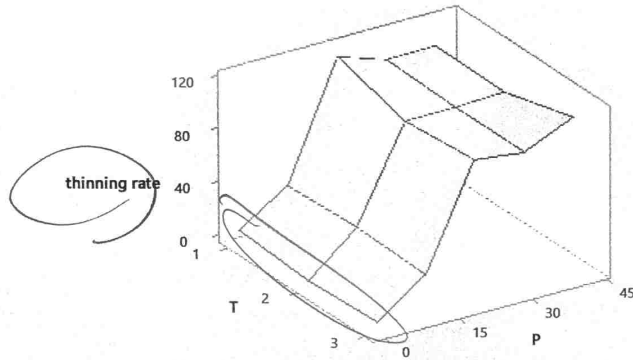
Regression Analysis.



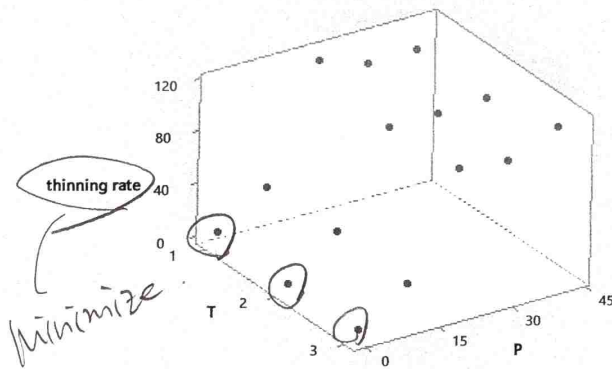
Appendix D Regression Analysis – Regression Plots 3D

Regression Analysis

Surface Plot of thinning rate vs P, T

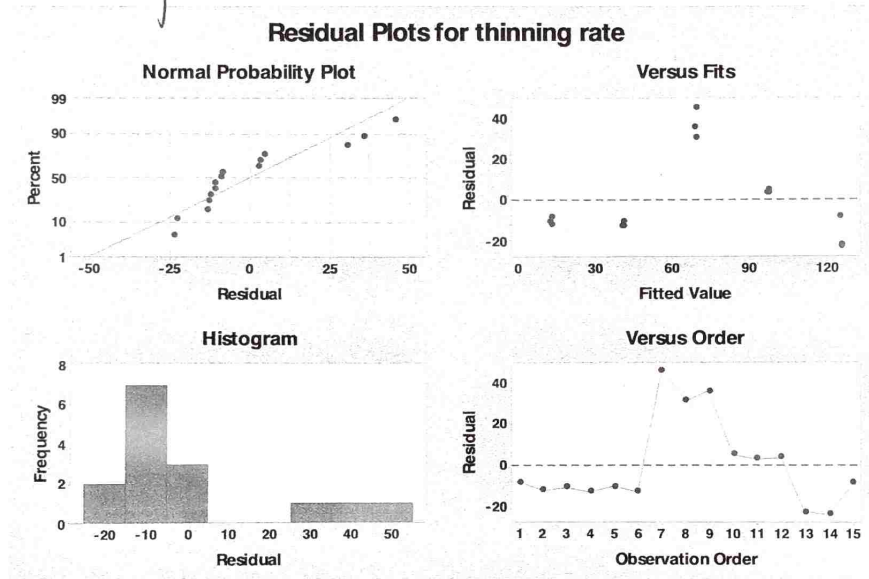


3D Scatterplot of thinning rate vs P vs T



Appendix E Regression Analysis – Residual Plots

Regression Analysis.



Appendix F General Factorial Regression with 54 Runs

NOT USING Binary Regression Equation.

General Factorial Regression: Results versus Pressure, Meshing, Time

Factor Information

Factor	Levels	Values
Pressure	6	0, 10, 20, 30, 40, 50
Meshing	3	5, 10, 15
Time	3	1, 2, 3

Analysis of Variance

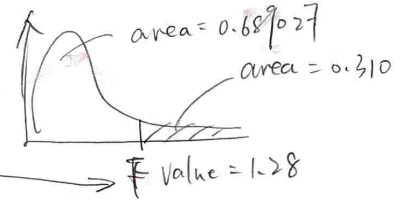
Source	DF	Adj SS	Adj MS	F-Value	P-Value
Model	33	5598244	169644	1.20	0.336
Linear	9	1749072	194341	1.38	0.261
Pressure	5	940102	188020	1.34	0.290
Meshing	2	474781	237390	1.69	0.211
Time	2	334189	167094	1.19	0.326
2-Way Interactions	24	3849172	160382	1.14	0.387
Pressure*Meshing	10	1668784	166878	1.19	0.356
Pressure*Time	10	1457324	145732	1.03	0.451
Meshing*Time	4	723064	180766	1.28	0.310
Error	20	2816220	140811		
Total	53	8414464			

main effect

2way interactions

$\alpha = \text{type I Error}$

not significant $\alpha = 0.05$



$5 \times 2 \times 2 = 20$

Model Summary

S	R-sq	R-sq(adj)	R-sq(pred)
375.248	66.53%	11.31%	0.00%

Coefficients

Term	Coef	SE Coef	T-Value	P-Value	VIF
Constant	117.5	51.1	2.30	0.032	
Pressure					
0	-110	114	-0.97	0.346	1.67
10	-98	114	-0.86	0.402	1.67
20	283	114	2.48	0.022	1.67
30	-47	114	-0.41	0.685	1.67
40	-9	114	-0.08	0.937	1.67
Meshing					

% Contribution of SS

pressure $\frac{940102}{8414464} = 11.2\%$
 mesh 0
 time 0

Error:

$\frac{100}{\%}$

5	-87.6	72.2	-1.21	0.239	1.33
10	-42.4	72.2	-0.59	0.564	1.33
Time					
1	111.2	72.2	1.54	0.139	1.33
2	-57.0	72.2	-0.79	0.439	1.33
Pressure*Meshing					
0 5	90	161	0.56	0.583	2.22
0 10	37	161	0.23	0.819	2.22
10 5	75	161	0.46	0.649	2.22
10 10	51	161	0.32	0.754	2.22
20 5	-300	161	-1.86	0.078	2.22
20 10	-252	161	-1.56	0.135	2.22
30 5	26	161	0.16	0.874	2.22
30 10	73	161	0.45	0.657	2.22
40 5	27	161	0.17	0.867	2.22
40 10	41	161	0.25	0.802	2.22
Pressure*Time					
0 1	-104	161	-0.65	0.525	2.22
0 2	51	161	0.32	0.753	2.22
10 1	-107	161	-0.67	0.513	2.22
10 2	54	161	0.34	0.740	2.22
20 1	517	161	3.20	0.004	2.22
20 2	-246	161	-1.52	0.144	2.22
30 1	-108	161	-0.67	0.510	2.22
30 2	55	161	0.34	0.735	2.22
40 1	-66	161	-0.41	0.688	2.22
40 2	13	161	0.08	0.935	2.22
Meshing*Time					
5 1	-122	102	-1.19	0.247	1.78
5 2	52	102	0.51	0.614	1.78
10 1	-109	102	-1.07	0.297	1.78
10 2	55	102	0.54	0.595	1.78
Regression Equation					

Math Model

$$\begin{aligned}
 \text{Results} = & 117.5 - 110 \text{ Pressure}_0 - 98 \text{ Pressure}_{10} + 283 \text{ Pressure}_{20} - 47 \text{ Pressure}_{30} \\
 & - 9 \text{ Pressure}_{40} - 19 \text{ Pressure}_{50} - 87.6 \text{ Meshing}_5 - 42.4 \text{ Meshing}_{10} \\
 & + 130.0 \text{ Meshing}_{15} + 111.2 \text{ Time}_1 - 57.0 \text{ Time}_2 - 54.2 \text{ Time}_3 \\
 & + 90 \text{ Pressure} * \text{Meshing}_0 5 + 37 \text{ Pressure} * \text{Meshing}_0 10 - 128 \text{ Pressure} * \text{Meshing}_0 \\
 & 15 + 75 \text{ Pressure} * \text{Meshing}_{10} 5 + 51 \text{ Pressure} * \text{Meshing}_{10} 10 \\
 & - 126 \text{ Pressure} * \text{Meshing}_{10} 15 - 300 \text{ Pressure} * \text{Meshing}_{20} 5 \\
 & - 252 \text{ Pressure} * \text{Meshing}_{20} 10 + 551 \text{ Pressure} * \text{Meshing}_{20} 15 \\
 & + 26 \text{ Pressure} * \text{Meshing}_{30} 5 + 73 \text{ Pressure} * \text{Meshing}_{30} 10 \\
 & - 99 \text{ Pressure} * \text{Meshing}_{30} 15 + 27 \text{ Pressure} * \text{Meshing}_{40} 5 \\
 & + 41 \text{ Pressure} * \text{Meshing}_{40} 10 - 68 \text{ Pressure} * \text{Meshing}_{40} 15 \\
 & + 82 \text{ Pressure} * \text{Meshing}_{50} 5 + 49 \text{ Pressure} * \text{Meshing}_{50} 10 \\
 & - 131 \text{ Pressure} * \text{Meshing}_{50} 15 - 104 \text{ Pressure} * \text{Time}_0 1 + 51 \text{ Pressure} * \text{Time}_0 2 \\
 & + 53 \text{ Pressure} * \text{Time}_0 3 - 107 \text{ Pressure} * \text{Time}_{10} 1 + 54 \text{ Pressure} * \text{Time}_{10} 2 \\
 & + 53 \text{ Pressure} * \text{Time}_{10} 3 + 517 \text{ Pressure} * \text{Time}_{20} 1 - 246 \text{ Pressure} * \text{Time}_{20} 2 \\
 & - 271 \text{ Pressure} * \text{Time}_{20} 3 - 108 \text{ Pressure} * \text{Time}_{30} 1 + 55 \text{ Pressure} * \text{Time}_{30} 2 \\
 & + 53 \text{ Pressure} * \text{Time}_{30} 3 - 66 \text{ Pressure} * \text{Time}_{40} 1 + 13 \text{ Pressure} * \text{Time}_{40} 2 \\
 & + 52 \text{ Pressure} * \text{Time}_{40} 3 - 131 \text{ Pressure} * \text{Time}_{50} 1 + 71 \text{ Pressure} * \text{Time}_{50} 2 \\
 & + 60 \text{ Pressure} * \text{Time}_{50} 3 - 122 \text{ Meshing} * \text{Time}_5 1 + 52 \text{ Meshing} * \text{Time}_5 2 \\
 & + 69 \text{ Meshing} * \text{Time}_5 3 - 109 \text{ Meshing} * \text{Time}_{10} 1 + 55 \text{ Meshing} * \text{Time}_{10} 2 \\
 & + 54 \text{ Meshing} * \text{Time}_{10} 3 + 231 \text{ Meshing} * \text{Time}_{15} 1 - 107 \text{ Meshing} * \text{Time}_{15} 2 \\
 & - 124 \text{ Meshing} * \text{Time}_{15} 3
 \end{aligned}$$

Fits and Diagnostics for Unusual Observations

Obs	Results	Fit	Resid	Std Resid	
19	15	519	-504	-2.21	R
22	115	626	-510	-2.24	R
25	2956	1941	1015	4.44	R
26	190	672	-482	-2.11	R
27	100	633	-533	-2.33	R

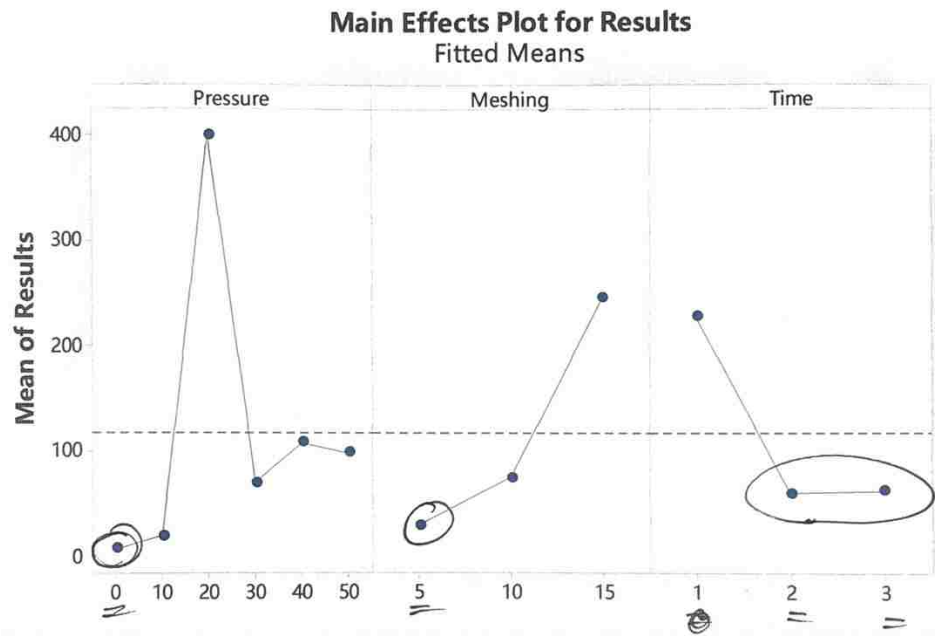
R Large residual

Effects Pareto for Results

Residual Plots for Results

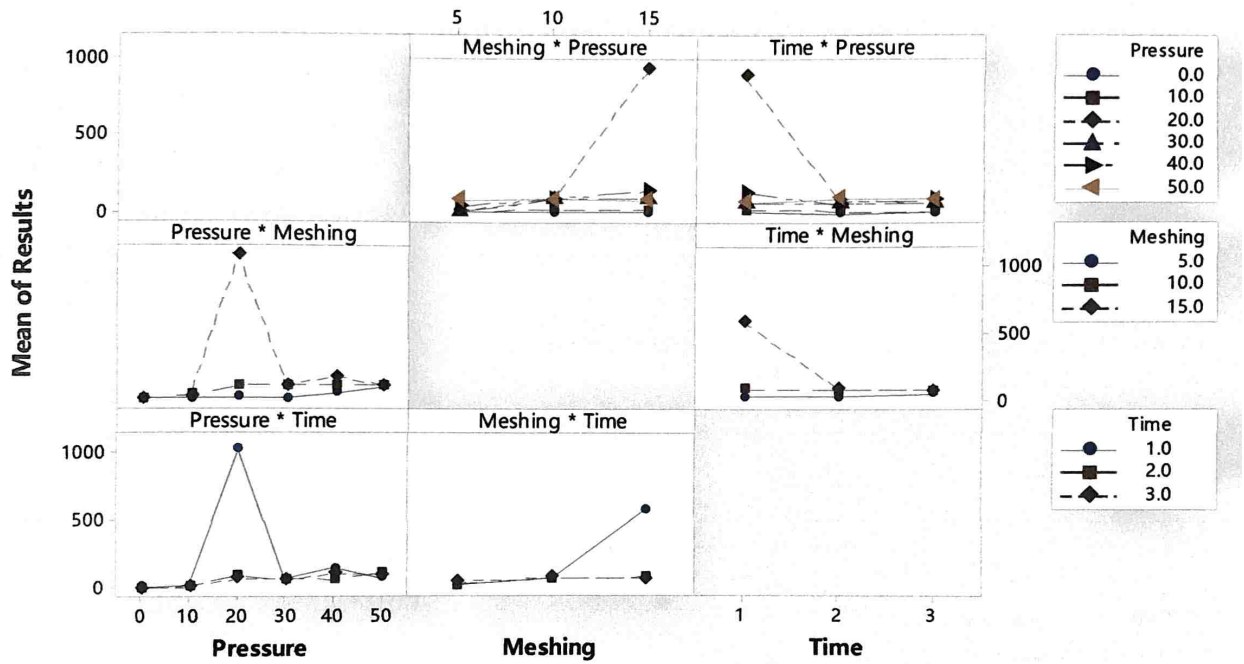
NO 3 way interaction
main effect + 2 way interaction

Appendix G General Factorial Regression – Plots

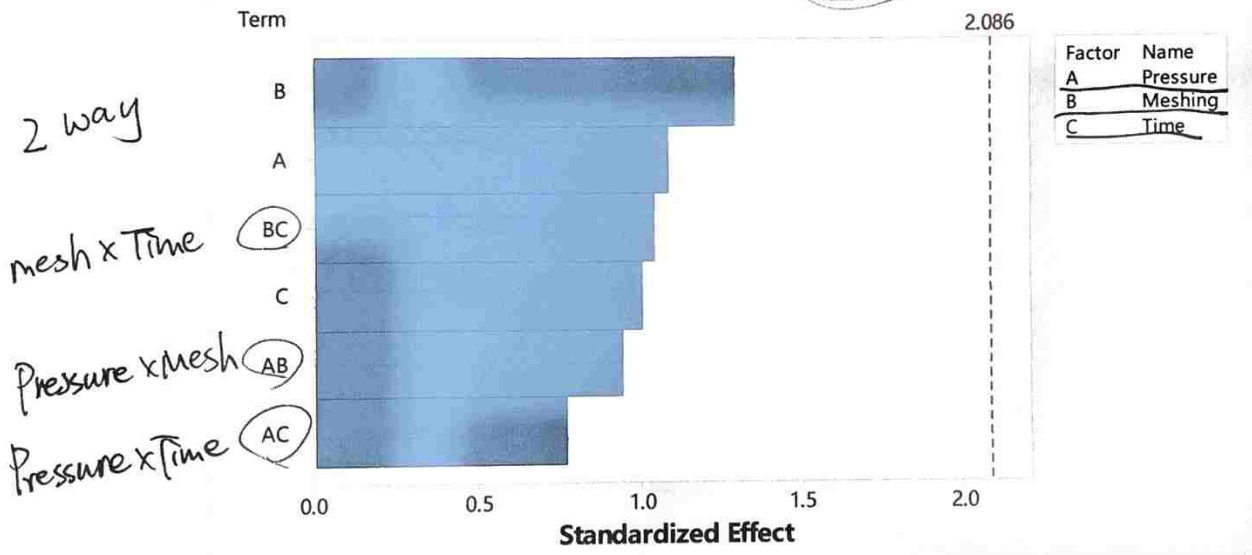


minimize results.

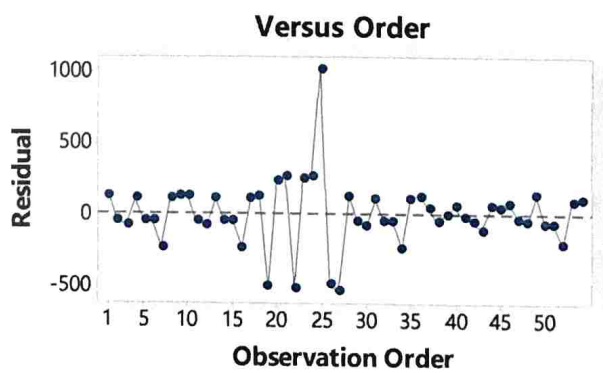
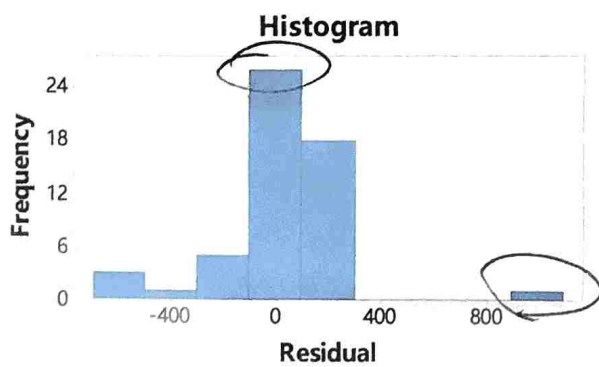
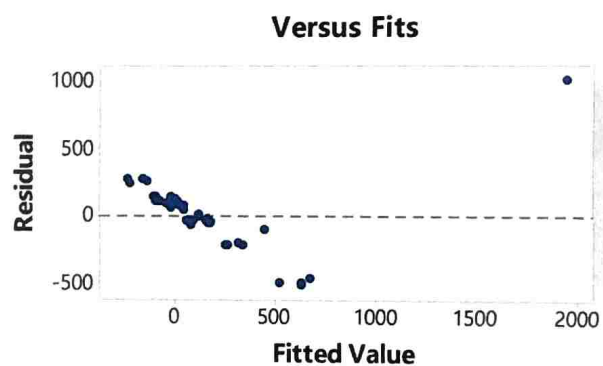
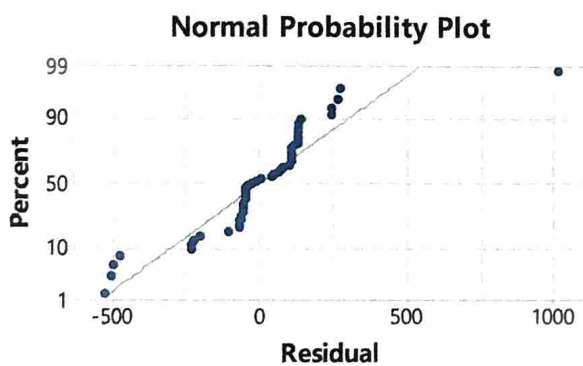
Interaction Plot for Results Fitted Means



Pareto Chart of the Standardized Effects
(response is Results, $\alpha = 0.05$)



Residual Plots for Results



Vita Auctoris

NAME: Yang Jin

PLACE OF BIRTH: Chongqing, China

YEAR OF BIRTH: 1992

EDUCATION: University of Windsor, Windsor, ON,
2012-2017 B.Sc.

University of Windsor, Windsor, ON,
2017-2019 M.A.Sc.